Design and performance of a toluene-degrading differential biotrickling filter as an alternative research tool to column reactors

Roger Jay L. De Vela[1] and Peter Alan Gostomski[2]

[1] Assistant Professor, Camarines Norte State College, F. Pimentel Ave., Daet, Camarines Norte, Philippines, 4600; https://orcid.org/0000-0002-5370-1113. Email: rogerjaydevela@gmail.com

[2] Professor, University of Canterbury, Christchurch, New Zealand, https://orcid.org/0000-0001-6001-7128. Email: peter.gostomski@canterbury.ac.nz

Abstract

A differential biotrickling filter (DBTF) was developed as a research tool to minimise radial and longitudinal gradients, which hinder analysis in integral (column) reactors. The main design modifications were a very high gas recycle rate and a low, uniform liquid addition rate via an aerosol generator. The elimination capacity (EC), uniformity of biofilm formation and long-term reliability of the reactor were evaluated. The maximum toluene elimination capacity was approximately 430 g/m^{3}h, which was higher than the EC in most previous reports. The high EC was potentially due to the thin liquid film over the biofilm generated by low liquid trickling rates. Moreover, the high gas recycle rate (2.5 – 100x the feed flow rate) allowed uniform substrate and nutrients distribution throughout the bed hence promoting favourable growth and performance of the microbes. These findings can serve as a guide in improving performance of industrial biotrickling filters. Substrate inhibition was observed at loading rates (LRs) higher than 513 ± 27 g/m^{3}h.

Despite operational issues that affected its long-term reliability, such as: (1) unwanted growth of microbes on the pipes and in the aerosol reservoir; (2) decline in the performance

of the aerosol generator; and (3) limited fan capacity, the DBTF is a promising tool that can improve biofiltration research.

Keywords: biotrickling filter, differential reactor, biofiltration, reactor development, substrate inhibition, biofilter

1 Introduction

Most biotrickling filter (BTF) studies employ column (integral) reactors (San-Valero et al. 2014, Liu et al. 2015, Wang et al. 2014, Ryu et al. 2010) where radial and axial variability in contaminant concentration, bacterial community and biofilm thickness are common (Cabrol et al. 2012b, Giordano et al. 2018). This motivated the current work to develop a DBTF as a research tool to investigate the physical, chemical and biological mechanisms in biofiltration. The DBTF described here is the first differential BTF that operates continuously. The DBTF of Kim and Deshusses (2005) operates in a batch mode while that of Beuger and Gostomski (2009) is a conventional biofilter with a stationary aqueous phase. This section describes the features of DBTF and the assumptions and principles considered in its development. Succeeding sections discuss the actual performance in terms of biofilm formation, elimination capacity (EC) and the operational problems (Sections 2 – 3).

1.1 Reactor development

A differential reactor minimises gradients in concentration, temperature, moisture, etc. by making the conversion per pass as small as possible (Carberry 1964) which leads to easier analysis of experimental data and performance (Cooper and Jeffreys 1971). Carberry (1964) discusses that only a continuous, stirred tank reactor (CSTR) possesses the ideal

characteristics of isothermal operation over a wide range of steady state conversions. Using the characteristics of a CSTR, a number of plug flow reactors that replicate the behavior of a CSTR have been developed including the recycle reactor (Carberry 1964) (Sec. 1.2).

The DBTF reactor developed here was a packed bed reactor which approximated the behavior of an ideal plug flow reactor. The DBTF bed thickness ranged from 10 to 50 mm, from which EC of 80 g/m^{3}h, RE of 50% (Supplemental information 3) and air flow rate of 0.84 L/min were subsequently chosen for subsequent design calculations. A short bed was chosen to minimise liquid maldistribution through the bed, as Mohammed et al. (2015) demonstrated with both a multipoint distributor and a spray nozzle that liquid uniformity declined with increasing bed length.

1.2 The recycle reactor

Carberry (1964) proposed that in a recycle reactor, CSTR behaviour is achieved by mixing the high rate recycle stream with the fresh feed, hence diluting the latter, leading to minimal conversion per pass. This assures negligible interphase, axial and radial gradients in a reactor. The components of the recycle reactor for the DBTF described in this paper included the packed bed, a fan for gas recycling and piping that formed the recycle loop (Fig. 1).

where:

C_{in} = toluene concentration of the inlet feed, g/m^3

$V_{g\ in}$ = volumetric flow rate of the inlet feed, m^3/h

C_1 = toluene concentration in the headspace, g/m^3

V_1 = volumetric flow rate entering the bed, m^3/h

C_2 = toluene concentration exiting the bed, g/m^3

69 V_2 = volumetric flow rate exiting the bed, m^3/h

70 V_R = gas recycle rate, m^3/h

71 C_{out} = toluene concentration of the outlet gas, g/m^3

72 V_{out} = volumetric flow rate of the outlet gas, m^3/h

73 $V_{l\,in}$ = volumetric flow rate of the incoming liquid phase, m^3/h

74 $V_{L\,out}$ = volumetric flow rate of the outgoing liquid phase, m^3/h

75

76 Design parameters like the recycle rate and ratio were assumed and/or calculated.
77 Assuming a toluene EC of 80 g/m^3h and an inlet concentration of 1 g/m^3, calculations
78 (Supplemental information 1) based on a recycle ratio of 20, generated a recycle rate of
79 17 L/min, toluene removal per pass of approximately 3% and an 8 ppm concentration
80 gradient across the bed. High flow rate was desired as it ensured negligible gas phase
81 gradients (Ranasinghe and Gostomski 2003). Hence the higher the gas recycle rate, the
82 smaller the concentration gradient across the bed.

83 **1.3 Choice of packing material and mode of operation**

84 Since the DBTF was envisioned to be used for future biomass control investigations,
85 it was necessary that the packing material support adequate microbial growth and minimise
86 maldistribution of liquid (Chen et al. 2006), features met by glass beads. Glass beads were
87 suitable in investigating bacterial adhesion on solid surfaces due to their chemical stability
88 and high reproducibility (Tsuneda et al. 2003). The amount of biomass supported by 2-mm
89 and 5-mm glass beads was estimated based on the biomass production (1.4 g of biomass per
90 m^2 of bed) and specific activity of biomass (0.05 mg of toluene degraded per mg of biomass
91 per hour) as measured by Mirpuri et al. (1997) (Supplemental information 3). Although 2-

92 mm glass beads yielded more biomass per unit volume of bed and higher EC, preliminary
93 tests revealed that its low void volume resulted in higher pressure drop across the bed, which
94 decreased recycle flow and aerosol delivery rate. Hence, 5-mm glass beads were chosen.
95 Co-current, down flow operation was preferred because countercurrent gas–liquid
96 flow in BTFs was unsuitable with 1 – 5 mm particles (Mederos et al. 2009). This was due to
97 the potential flooding problem in the counter current configuration initially observed when
98 using 5-mm glass beads.
99 **1.4 Operational conditions**
100 The major operational parameters affecting the EC in a BTF were inlet concentration
101 (C_{in}), gas flow rate (V_g), and liquid flow rate (V_l). Representative values (Table 1) were used
102 in estimating the reactor size and potential EC. Based on the C_{in} employed in previous BTFs,
103 C_{in} of 1 g/m^3 was used in designing the diffusion system for the DBTF .
104 **1.4.1 Gas flow rate**
105 In a recycle reactor, liquid distribution and mass transfer of the contaminant to the
106 biofilm could be greatly influenced by the gas recycle rate (V_R) (Fig. 1). The effect of gas
107 velocity (V_g) on liquid distribution and mass transfer coefficients varied among different
108 studies. Maldistribution of liquid in the radial and axial directions in multiphase reactors
109 results in a fraction of the packing having little to no liquid causing reduced activity (Maiti
110 et al. 2004). Goto and Smith (1975) and Mohammed et al. (2015) observed that gas velocity
111 did not significantly influence liquid maldistribution and the gas–to–liquid mass transfer
112 coefficient (k_La). However, others demonstrated that the volumetric mass transfer coefficient
113 was affected either by the liquid or the gas phase velocities (Kim and Deshusses 2008, Liu
114 et al. 2015, Perez et al. 2006, Wang et al. 1998).

115 Wang et al. (1998) observed that small–scale maldistribution was governed by gas –
116 liquid interaction while large–scale maldistribution was controlled by solid – liquid
117 interaction. Hence, the ratio V_g/V_l which ranged by 5-orders of magnitude in toluene-
118 degrading BTFs (Table 1) suggested their combined effect on mass transfer. Different V_g/V_l
119 values were examined to determine the appropriate operational conditions for the DBTF (V_g
120 and V_l).

121 **1.4.2 Liquid flow rate**

122 The liquid flow rate also affected the size of the collector tank and/or whether a single
123 pass of liquid was practical over recycling the liquid back to the reactor. Liquid recycle was
124 avoided because toluene degradation in the liquid could contribute up to 21% of the total EC
125 (Cox et al. 2000) and to ensure that EC measurements represented only the degradation in
126 the biofilm.

127 A gas recycle rate of 5 – 30 L/min and V_g/V_l ratio of approximately 1,000 yielded
128 liquid flow rates of about 5 – 30 mL/min. This involved up to 45 L of potential waste liquid
129 per day. With this small amount of liquid, single-pass flow was practical, thereby eliminating
130 the need for liquid recirculation.

131 **1.5 The liquid distribution system**

132 Based on Section 1.4.2, options explored for the liquid distribution system included:
133 (1) hydraulic spray nozzle; (2) pneumatic/air atomizing nozzle or nebulizer; (3) vibrating
134 mesh or plate for aerosol production (4) centrifugal atomizer and (5) ultrasonic atomization.
135 Although its trickling rate was lower than the desired value, ultrasonic atomization yielded
136 uniform liquid distribution and was chosen for the liquid distribution system of the DBTF. A
137 three-disc ultrasonic aerosol generator (The House of Hydro, USA) was used for the final

DBTF system (Sec. 1.7). It is the second BTF to use ultrasonic aerosol generation to supply nutrients to a BTF after Song and Kinney (2000).

1.6 The diffusion system

A continuous supply of toluene-contaminated air to the DBTF reactor was ensured through a diffusion system capable of generating varying concentration of toluene in air. In a diffusion system, toluene was vaporized into the diluent gas through a capillary tube, eventually mixing it with the diluent gas to produce a desired concentration (Altshuller and Cohen 1960). The design of the diffusion system for the DBTF was based on the work of Detchanamurthy and Gostomski (2013) and was governed by parameters such as temperature of the water bath, gas flow rate and geometry of the diffusion tube.

At water bath temperatures ranging from 25 °C to 50 °C, the resulting concentration deviated about 2 – 6% from the theoretical values while that at lower temperatures deviated by approximately 4 – 16% (Fig. S1, Supplemental information 2). Similar diffusion systems in the literature yielded 5 – 10% difference between actual and theoretical values (McKelvey and Hoelscher 1957, Nelson 1971), hence the deviations obtained from the current diffusion system were reasonable.

1.7 The final design

Based on the different components and the design requirements discussed in the preceding sections, the final DBTF design consisted of the reactor bed, aerosol generator, recirculation fan and feed reservoir connected to each other using stainless steel pipes (Fig. 2). The reactor bed consisted of the top (1) and bottom (2 and 3) sections (Fig. S7; Supplemental information 2). The bottom glass pipe enabled visual inspection of the interior

during the run. The head plate of the DBTF had a port for recycle gas entry. In addition, it also had three ports: two served as inlet and outlet gas ports and one as a thermo-well.

The lower half of the bottom portion (3) made of stainless steel consisted of a funnel-shaped base to easily drain liquid via a valve. A stainless steel pipe connected the bottom portion of the reactor to the glass reservoir, hence forming part of the recycle gas path. The plate which served as the base of the whole reactor was supported by three threaded rods.

Inside the glass reservoir of nutrient medium was a three-disc ultrasonic aerosol generator (House of Hydro) capable of producing aerosol (10 – 15 μm) at a maximum rate of 25 mL/min (Fig. S8; Supplemental information 2). An external nutrient reservoir connected to the system through a stainless steel tube based on a simplified version of the 'inverted water bottle' used by Burrhus and Hart (1972) ensured adequate amount of medium in the reservoir. The maximum amount of nutrient delivered to the bed was only up to 1.75 mL/min at a gas recycle of 250 L/min in a 50-mm deep bed (Fig. S11; Supplemental information 2). Further increases in the gas recycle did not significantly increase the aerosol coalescence, potentially due to the aerosol hitting the pipe wall and dripping down back the aerosol reservoir. The fan used to deliver the aerosol to the bed was an IP68 axial fan (San Ace, USA) operated at varying speeds and pressure drops from 3,000 to 11,000 RPM (Fig. S2, Supplemental information 2).

2 Materials and methods

2.1 Overall description of the DBTF system

Feed air was passed through the diffusion system to generate toluene-laden air for the DBTF reactor. This gas was recycled by the fan at a rate determined by the pressure drop in the system and the fan speed. Nutrients were supplied to the bed as aerosol transported by

183 the recycle gas. The aerosol was generated ultrasonically and an external reservoir ensured
184 that the aerosol reservoir was constantly provided with fresh medium. Carbon dioxide was
185 determined with a Vaisala CARBOCAP Carbon Dioxide Probe GMP 343 (Vaisala, Finland).
186 An on-line gas chromatograph (8610 SRI Instruments) (SRI Instruments, USA) was used for
187 toluene gas analysis (Fig. 3).

188 **2.1 Leak testing and abiotic losses**

189 Leak tests used a combination of (1) inlet and outlet flow measurement; (2) bubble
190 tests using Snoop (Swagelok); (3) G3388B electronic leak detector (Agilent, USA); and (4)
191 pressure change/decay method by pressurizing to 7.10 kPa. Before inoculation, an abiotic
192 loss test was done, where the DBTF was fed with 0.42 ± 0.01 g/m^3 toluene at 0.84 L/min.
193 Inlet and outlet toluene concentrations were monitored for seven days and the difference
194 between the two values indicated the abiotic losses through the system.

195 **2.2 Inoculation and start-up**

196 The inoculant used for the DBTF system was from a column BTF which was
197 degrading toluene for over 100 days. Approximately 100 mL of the liquid from the seed
198 reactor was sprayed onto the 0.40 L DBTF bed using a Masterflex console-drive peristaltic
199 pump (Masterflex, Thermo Fisher Scientific New Zealand Ltd). It was collected at the bottom
200 of the liquid sump and recirculated back to the bed until sufficient wetting was achieved
201 (~ 2 h).

202 The DBTF was acclimated using a LR of about 60 g/m^{3}h for 10 days. Throughout the
203 run, the reactor bed was supplied with nutrient solution in the form of aerosol at a rate
204 determined by the recycle gas. The nutrient medium was similar to that used by Shen et al.
205 (1998) composed of (g/L): 4 $NaNO_3$; 2.6 NaH_2PO_4; 1.2 K_2HPO_4; 0.0008 $FeSO_4 \cdot 7H_2O$; 0.2

206 $MgSO_4 \cdot 7H_2O$; 0.009 $CaCl_2 \cdot 2H_2O$ with trace elements based on Dedysh and Dunfield (2014)
207 (g/L): 0.2 $FeSO_4 \cdot 7H_2O$; 0.01 $ZnSO_4 \cdot 7H_2O$; 0.003 $MnCl_2 \cdot 7H_2O$; 0.02 $CoCl_2 \cdot 6H_2O$; 0.002
208 $NiCl_2 \cdot 6H_2O$; 0.03 $CuSO_4 \cdot 5H_2O$; 0.003 Na_2MoO_4; 0.03 H_3BO_3; 0.5 Na_2EDTA.

209 **2.3 Analytical methods**

210 **2.3.1 Gas phase analysis**

211 Inlet and outlet gas streams were sampled via a 22-port stream selector valve then to
212 a 10-port valve for sample injection and finally to the GC/FID (SRI-8610C, SRI Instruments,
213 USA). The 10-port valve contained a 1-mL sample loop. This volume was injected on to the
214 60-m MXT-1 capillary column (Restek Corporation, USA). The GC was operated with
215 33 mL/min carrier gas flow (He), 250 mL/min air flow, and 25 mL/min hydrogen flow at a
216 FID temperature of 200 °C while maintaining the column temperatures at 200 °C. Both the
217 inlet and outlet lines of the reactor systems were measured in triplicate every day and
218 compared to a regularly-updated calibration curve. EC and removal efficiency (RE) were
219 calculated daily.

220 The inlet and outlet CO_2 content were measured using a Vaisala CARBOCAP Carbon
221 Dioxide Probe GMP 343 (Vaisala, Finland) calibrated every three months. The CO_2 probe
222 was connected to the purge port of the sample loop of the GC. The CO_2 content of the inlet
223 line was subtracted from the outlet CO_2 and combined with toluene degradation to determine
224 the $\%CO_2$ recovery.

225 **2.3.2 Carbon content in the liquid sump, aerosol reservoir, pipes and bed**

226 The total organic carbon (TOC) contained in the liquid sump of the DBTF represented
227 the organic carbon released by the biomass in the bed. A 15-mL liquid sample was collected
228 from the liquid sump and its TOC was measured in triplicate using a TOC-L analyzer

(Shimadzu, USA) liquid module and Shimadzu SSM 5500 solid module for low and high solids liquid samples, respectively.

The TOC in the bed and recycle pipes was also measured. The biomass samples from the bed were obtained by scraping biofilm from the beads using a spatula and were added to 50 mL of fresh medium. For the pipes, biomass samples were collected by passing a test tube brush through them until completely clean and then added to 200-mL of fresh medium. Ten mL of each sample was transferred to a 15-mL centrifuge tube and was vortexed using a PCV-2400 Grant-bio vortex mixer (Grant, United Kingdom) at a maximum of 2,800 rpm speed for approximately 1 minute to ensure a more homogenous mixing of the biomass samples.

Biomass samples from the aerosol reservoir and liquid sump were directly collected from their corresponding drain plugs. Aside from TOC, the growth of microorganisms in the aerosol reservoir was monitored by measuring absorbance (600 nm) using an Ultrospec 2100 pro UV/Visible spectrophotometer (Biochrom, United Kingdom).

2.3.3 Column reactor

The performance of the DBTF was compared to a column reactor (i.e. control) in terms of biofilm development, EC and RE. The latter consisted of an acrylic tube packed with 5-mm glass beads to a volume of 0.45 L, employing a co-current flow of trickling liquid and toluene-contaminated air. Nutrient medium was added at a rate of 24 ± 1 mL/min through a four-port nozzle and recirculated through the bed using a Masterflex 7018-20 pump head and L/S 18 Norprene tubing. The air flow rate was 0.84 L/min and empty bed residence time (EBRT) was 32 ± 0.4 s.

2.3.4 Testing the validity of EC values

Actions were undertaken to confirm that the EC values of the DBTF were valid, including: (1) cleaning of the pipes and adding fresh liquid medium to the aerosol reservoir; (2) measuring the TOC of the biomass samples from different portions of the system; and (3) measuring the EC after bed removal.

The pipes were cleaned and the liquid medium was replaced (day 31) to determine if their biomass contributed to the EC. The system was reassembled and was fed 430 g/m^3h toluene. EC was monitored to test if the removal of the biomass from other portions of the system would result to drop in EC.

Moreover, the TOC of the biomass collected from different portions of the system on the 30^{th} and 100^{th} days of operation was measured and used for the estimation of their proportion relative to the biomass in the bed. The estimation assumed that only 50% of the pipes was covered with biofilm and that it was thinner (1-mm thickness) than that of the bed's biofilm (1.5 mm). The final test to confirm that the EC was due to the biofilm in the bed was the removal of the bed on day 132. After the removal, the change in EC was monitored.

3 Results and Discussion

The DBTF system was free of leakage and an abiotic loss of 2.0 ± 0.3 g/m^3h was observed and subtracted from all the succeeding EC measurements. The succeeding sections discuss the performance of the DBTF in terms of biofilm development, EC, substrate inhibition and the problems encountered during its operation.

3.1 Biofilm development in DBTF

The biofilm on the DBTF reactor developed rapidly over the first 25 days (Fig. 4). The amount of the biofilm on the reactor was evenly distributed throughout the radial and

axial directions in the DBTF, except for day 85 where the bed was unintentionally dried because of the failure of the aerosol generator.

The development of biofilm on the DBTF bed was more uniform than in the column reactor (Fig. 5) due to the uniform liquid distribution facilitated by aerosol addition (0.09 to 0.70 mL/min) in the former as compared to the sprinkling/dripping rate (24 ± 1 mL/min) achieved through a four-port nozzle in the latter (Fig. S3, Supplemental information 2). The latter emitted the liquid drop-wise, wetting only four distinct areas in top of the bed. In terms of liquid and nutrient distribution, the DBTF was closer to being an ideal reactor than its column counterpart. Mederos et al. (2009) described that in an ideal reactor, all catalyst particles equally contribute to the overall conversion which is possible when each is surrounded by the flowing film of liquid and exposed to the same flux of gas. In the column reactor, liquid preferentially flowed through certain parts of the bed specifically at its early stage (day 24). Liquid maldistribution was persistent in this system, causing a variability in the thickness of the biofilm as indicated by colour variation in the column. This liquid maldistribution may have been minimised had a fine spray nozzle been used (Cárdenas-González et al. 1999) but the minimum rated flow of spray nozzles in the market was > 100 mL/min which was ~ 10 times higher than the desired liquid trickling rate for the column and DBTF reactors (10 – 30 mL/min).

The non-uniform liquid flow through the column reactor likely caused preferential gas flow, which contributed to the non-uniform biofilm growth in the bed. On the contrary, liquid distribution was uniform throughout the DBTF bed thereby minimising channelling and causing the gas to flow uniformly throughout the bed. Hence, a more uniform biofilm growth.

297 Another reason for the biofilm uniformity in the DBTF was the short bed (50 mm)
298 which may have minimised the microbial diversity along the bed. Variability in microbial
299 diversity along a biofilter was demonstrated by Lepeuple et al. (2012) and Cabrol et al.
300 (2012b) where higher microbial diversity occurred in the gas inlet region due to the constant
301 availability of the contaminant.

302 **3.2 Elimination capacity**

303 Figure 6 shows the changes in the EC and operating conditions of the DBTF reactor
304 with time. In the DBTF reactor, the bed experienced the outlet concentration (i.e. residual
305 concentration) rather than the inlet concentration. Hence, the outlet concentration at varying
306 LR was monitored. After inoculation, the EC was only 5.3 g/m^3h at LR of about 63 g/m^3h
307 and an EBRT of 28 seconds. The EC from days 1 to 11 was not monitored due to GC issues
308 while days 34 – 54 corresponded to period of aerosol generator failure.

309 From day 12 to 16, the LR was 79 ± 4 g/m^3h, the RE was 97 ± 7% and the EC was
310 76 ± 9 g/m^3h. During this period, the outlet concentration was very low at 0.020 ± 0.002
311 g/m^3. Hence, the LR was gradually increased from 79 g/m^3h to 410 g/m^3h from day 17 to 30,
312 and the EC increased to 404 g/m^3h on day 30 and the outlet concentration was 0.11 ± 0.006
313 g/m^3. On day 32, the aerosol generator started failing and delivered less aerosol until it
314 eventually stopped the following day, gas flow was stopped, hence starving the bed for the
315 next 20 days (days 34 to 54). Normal operation resumed at day 55 with a LR of 518 ± 22
316 g/m^3h for the next 8 days (days 55 to 62). Despite the 20% increase in LR, the RE was at a
317 relatively high value of 80 ± 18% corresponding to fluctuating EC of 415 ± 104 g/m^3h and
318 an outlet concentration of 0.80 ± 0.72 g/m^3, thereby not achieving steady state. Since the
319 DBTF bed experienced the outlet concentration, the high outlet concentration resulting from

320 the increase in LR led to a hypothesis that there could be substrate inhibition at that stage of
321 the operation.

322 To test this, the LR was increased to 657 ± 64 g/m^{3}h (20% increase) from days 63 to
323 66 which then decreased the average RE to 42 ± 9% and yielded an EC of 272 ± 40 g/m^{3}h
324 and an increase in the outlet concentration to 3.0 ± 0.7 g/m^3. These results were consistent
325 with substrate inhibition where the DBTF could only achieve approximately 100% RE and
326 ~ 0 g/m^3 outlet concentration up to a LR of 430 g/m^{3}h of LR. To verify, the LR was reduced
327 to 197 ± 37 g/m^{3}h from days 67 to 71 and RE increased to 95 ± 4% yielding an EC of
328 187 ± 30 g/m^{3}h and an outlet concentration of 0.08 ± 0.08 g/m^3. The LR was again increased
329 to 583 g/m^{3}h (approximately 40% higher than the suspected optimum LR of 430 g/m^{3}h for a
330 day (day 72) which again decreased RE to 47% and increased the outlet concentration to 2.43
331 g/m^3, thus further strengthening the substrate inhibition hypothesis. The succeeding 17 days
332 (days 73 to 89) when the LR was 472 ± 70 g/m^{3}h saw an RE of 88 ± 13% which was still
333 high considering that LR exceeded the suspected maximum value. This translated to an
334 average EC of 414 ± 86 g/m^{3}h and outlet concentration of 0.45 ± 0.50 g/m^3. Substrate
335 inhibition is further discussed in Sec 3.4.

336 The gas recycle rate decreased from 83 to ~ 2 L/min over a period of 80 days and this
337 low recycle increased the concentration gradient across the bed, moving it away from
338 differential operation. Therefore, the bed thickness was reduced from 50 mm to 10 mm on
339 day 90, without changing the inlet concentration (4.2 ± 0.1 g/m^3) for two days, thereby
340 increasing the LR to 2680 ± 35 g/m^{3}h. Decreasing the bed thickness but keeping the gas flow
341 rate at 0.84 L/min decreased the EBRT from 28 seconds to approximately 6 seconds. RE
342 decreased to 59 ± 5% and EC increased to 1,310 ± 262 g/m^{3}h while the outlet concentration

343 was at 1.71 ± 0.24 g/m^3. After which, the LR was reduced to 364 ± 5 g/m^{3}h for the next three
344 days where RE increased again to 98 ± 2% and EC was at 318 ± 65 g/m^{3}h and outlet
345 concentration decreased to 0.01 ± 0.01 g/m^3. For days 95 to 102, the LR was increased to
346 580 ± 32 g/m^{3}h giving an EC of 567 ± 31 g/m^{3}h and an outlet concentration of 0.02 ± 0.01
347 g/m^3.

348 When bed thickness was 50 mm, the maximum EC demonstrated by the DBTF for
349 multiple days (430 g/m^{3}h) was 7 times higher than that of the column reactor (57 g/m^{3}h) and
350 up to 38 times higher than the typical EC (approximately 11 – 300 g/m^{3}h) in most reports
351 (Misiaczek et al. 2007, Weber and Hartmans 1996, Chen et al. 2012, Cox et al. 1998, Cox
352 and Deshusses 2002, Cox and Deshusses 1999, Singh et al. 2010, Chang and Lu 2003, He et
353 al. 2009, Lebrero et al. 2012, Sun et al. 2013, Zilli et al. 2001, Li et al. 2008). A high EC
354 (3,700 g/m^{3}h) was reported by Ryu et al. (2008) from a BTF using polyurethane as packing
355 where the high specific surface area, porosity and the ease of removal of excess biomass
356 through backwashing contributed to a high EC. Similarly, EC of 6,665 g/m^{3}h was achieved
357 in the biofilter of Kumar et al. (2019) with an inlet concentration of up to 37.4 g/m^3,
358 consisting of a bed of compost and activated carbon and was supplied with nutrients at a rate
359 of 0.002 m/h.

360 **3.2.1 Cleaning of the pipes and medium replacement**

361 After cleaning and reassembling the system and feeding it with 430 g/m^{3}h toluene,
362 no significant decrease in EC (408 g/m^{3}h) occurred indicating that the EC was primarily due
363 to the bed biofilm. This was further validated by the negligible EC change after the cleaning
364 operation on the 100th day.

365 **3.2.2 Biomass from different portions of the DBTF**

About 80% of the TOC in the system was in the bed while that of the pipe and in the aerosol reservoir were about 17 - 28% of the TOC in the system (Fig. S9, Supplemental information 2). This supported the hypothesis that the high EC of the system was mostly due to the bed. Although the biomass in the aerosol reservoir and in the pipe could have contributed to the total EC of the system like what was observed by Cox et al. (2000), the suspended biomass in their work was recirculated and therefore not a good comparison. In the DBTF, the liquid phase passed through the bed only once while the gas phase was recycled at a high rate (2 – 80 L/min), hence potentially resulting in different mass transfer kinetics. López de León et al. (2019) showed in their toluene-degrading miniaturized BTFs and capillary microbioreactor that over 89% of the EC (120 – 3,050 g/m^3h) was due to the bioreactor itself, not to the biodegradation in the liquid phase. The configuration of the capillary microbioreactor resulted in Taylor flow which increased the mass transfer of poorly soluble compounds like methane and oxygen (Rocha-Rios et al. 2013).

Since there was microbial growth in the aerosol reservoir as indicated by increasing absorbance of the medium (Fig. S5 Supplemental information 2), it could not be concluded that toluene removal from the aerosol reservoir and the pipes was insignificant. However, the favourable conditions in the bed may have caused the biofilm to be very active, therefore essentially complete toluene degradation was observed even after the removal of the biomass on the pipes and reservoir.

The $\%CO_2$ recovery was about 83 ± 33% indicating a small portion of the degraded toluene went to biomass. Some values exceeded 100% potentially due to the degradation of internal storage polymers (e.g. polyhydroxybutyrate), which may have been produced as a response to nutrient limitation (Thapa et al. 2019). These high $\%CO_2$ recovery values started

389 on day 32, the day after the disassembly and cleaning of the pipes and the aerosol reservoir,
390 which lasted 5 h. This may have caused substrate and nutrient limitation in the bed, prompting
391 the microbes to degrade accumulated PHB thereby releasing more CO_2 upon resumption of
392 normal operation. PHB may have also accumulated for about 20 days until day 55 due to the
393 failure of the aerosol generator. The %CO_2 recovery upon resumption of normal operation
394 was over 105%.

395 Finally, the removal of the bed on day 132 caused the EC of the system to drop from
396 205 g/m^3h to 5 g/m^3h (~ 98% drop). The aerosol reservoir was not replaced with fresh
397 medium and the pipes had not been cleaned for ~ 30 days when the bed removal was done,
398 thereby confirming that the EC contributed by the biomass in the pipes and the reservoir were
399 not significant.

400 **3.3 Factors contributing to high EC**

401 Two potential factors that contributed to high EC values were identified: (1) uniform
402 substrate and nutrient distribution throughout the bed and (2) a thin liquid film in the bed.
403 Uniform toluene and nutrient distribution across the bed was a result of the gas recycle and
404 may have favoured optimum growth and degradation performance of the biofilm similar to
405 that observed by Song and Kinney (2000) when directional switching biofilter was used
406 instead of a unidirectional biofilter where only one end was exposed to fresh toluene feed.
407 The former minimised the difference in microbial population density brought about by non-
408 uniform feed distribution and resulted in a population, which was twice as active as that of
409 the latter. Other BTF reports likewise showed that higher removal occurred at the inlet section
410 due to higher microbial activity (Cabrol et al. 2012a, Jiménez et al. 2016, López et al. 2013).

411 Similarly, non-uniform nutrient distribution by the four-port nozzle in the column
412 reactor may have caused portions of the bed to be nutrient-limited hence optimizing
413 degradation capacity. This was in contrast with the DBTF where the uniformly distributed
414 aerosol reached all portions of the bed, allowing uniform growth of microbes.
415 Meanwhile, the main resistance to toluene mass transfer to the biofilm was the liquid
416 film as estimated by Lebrero et al. (2012) from the Van Krevelen and Hoftijzer correlations
417 using a Henry's coefficient of 0.15 mol/L atm (Sander 2015). The low aerosol delivery rate
418 (0.09 to 0.70 mL/min) caused a thin liquid film in the bed which allowed easy transfer of
419 pollutant from the gas to the biofilm. Using the liquid flow rate in the column and DBTF
420 reactor, the liquid film thickness in the DBTF reactor (0.0002 to 0.002 mm) was estimated
421 to be 20 to 200 times thinner than that of the column reactor (0.04 mm). From the general
422 one-dimensional mass flux equation, the amount of toluene transferred from the liquid phase
423 to the biofilm was inversely proportional to the liquid film thickness. Hence, a greater
424 degradation at a lower liquid film thickness. Moreover, using the linear relationship between
425 toluene transfer capacity (TTC) and $k_L a$, and extending it beyond the V_g/V_l of 300 used in
426 the experiments of Lebrero et al. (2012), as well as using similar inlet concentration of toluene
427 for both BTFs, the TTC of DBTF (V_g/V_l > 100,000) was estimated to be at least 3,000 times
428 greater than that of the column BTF (V_g/V_l = 35).
429 From literature, high toluene EC values (100 – 6,700 g/m^{3}h) were obtained from
430 BTFs with superficial liquid velocities in the range of 0.001 – 0.07 m/h (Chang and Lu 2003,
431 He et al. 2009, Sun et al. 2013, Zilli et al. 2001, Li et al. 2008, Ryu et al. 2008, Kumar et al.
432 2019) while EC values < 100 g/m^{3}h were obtained from BTFs that had superficial liquid
433 velocities one to three orders of magnitude bigger (0.3 – 10 m/h) (Misiaczek et al. 2007,

Weber and Hartmans 1996, Cox et al. 1998, Chen et al. 2012, Cox and Deshusses 2002, Cox and Deshusses 1999, Singh et al. 2010). This further strengthened the hypothesis that the low liquid velocity in the DBTF (0.0007 - 0.005 m/h) yielding a thin liquid film on the bed contributed to its high EC. However, more work on the effect of liquid trickling rate is required to confirm this hypothesis.

3.4 Substrate inhibition

Evaluating the EC and outlet concentration at varying LRs, the DBTF demonstrated two regions: the diffusion-limited region (1) and reaction-limited region (2) (Fig. 7), similarly observed in many biofilter operations (Jorio et al. 2000, Krailas et al. 2000, Shukla et al. 2011). At a constant gas feed rate of 0.84 L/min, the diffusion-limited region extended up to LR of 514 ± 27 g/m^3h. In this region, the EC was directly proportional to the LR as more of the biofilm was active (Ottengraf and Vandenoever 1983).

Further increase in LR decreased the EC and increased the outlet concentration. Such a decrease in EC with increasing LR was potentially due to the inhibitory effect of higher pollutant concentration as observed by other researchers (Hwang and Tang 1997, Krailas et al. 2000, Shukla et al. 2011). Hwang and Tang (1997) who worked with toluene observed that a concentration of 3.32 – 4.92 g/m^3 caused substrate inhibition while Rene et al. (2005) recorded ~ 2.3 g/m^3, close to the inhibitory outlet concentration of 2.25 – 3.78 g/m^3 observed in this study. The DBTF was a good tool in analysing substrate inhibition in a BTF due to the uniform condition across the bed. It overcame the variability observed in the column reactor as indicated by non-uniform biofilm growth observed in the latter. However, operational problems caused temporal changes in terms of liquid and nutrient delivery rate as discussed below.

3.5 Operational problems encountered

Issues in the operation of the DBTF include: (1) biomass accumulation on the pipes and in the aerosol reservoir; (2) aerosol generator stability; and (3) limited fan capacity. Toluene and nutrients recirculation led to growth of microorganisms in the pipes and aerosol reservoir (Fig. S6, Supplemental information 2). The continuous operation of the aerosol generator produced heat hence increasing the temperature of the medium from 23 °C to ~ 40 °C. Although it was shown that these portions did not significantly contribute to the overall EC (Sec. 3.2), regular cleaning ensured that growth would not become excessive and would not hamper DBTF performance.

The failure of the aerosol generator on day 33 was due to continuous operation which increased the temperature in the reservoir to ~ 40 °C, causing it to draw more current and blow the fuse. Therefore, a cooling coil was added to the reservoir to maintain the temperature at ~ 20 °C thereby preventing overheating during continuous operation. In addition, biofilm accumulated on the disks which affected performance and required periodic cleaning.

Meanwhile, the increased pressure drop across the DBTF bed reduced the recycle gas flow and aerosol delivery throughout its long-term operation. Hence, a fan or a configuration with greater dynamic pressure capacity would improve the reliability of the DBTF system and would enable tests to understand how each of the operational parameter affected its performance. A two-fan-in-series configuration was tested and doubled the pressure capacity of the system, thereby enabling wider operating capacities in the future (Fig. S2, Supplemental information 2).

4 Conclusions

The remarkably high EC of the DBTF was primarily from the bed and due to the thin liquid film caused by low liquid trickling rate in the form of aerosol and uniform distribution of substrate and nutrient that encouraged favourable growth and performance of the microbes. The DBTF exhibited diffusion and reaction-limited regimes and was a promising research tool that can minimise gradients observed in a column BTF. Its long-term reliability was limited by: (1) growth of microbes on the pipes and in the aerosol reservoir; (2) decline in the performance of the aerosol generator with time; and (3) limited fan capacity.

Supplemental information

Data Availability

All data, models, and code generated or used during the study appear in the submitted article.

References

Altshuller A.P. and Cohen I.R. 1960 "Application of diffusion cells to the production of known concentrations of gaseous hydrocarbons." *Anal. Chem.* 32 (7): 802-810.

Beuger A.L. and Gostomski P.A. 2009 "Development of a biofilter with water content control for research purposes." *Chem. Eng. J.* 151 (1-3): 89-96.

Burrhus K.D. and Hart S.R. 1972 "Constant-level liquid feed-control for high purity distillation apparatus." *Anal. Chem.* 44 (2): 432.

Cabrol L., Malhautier L., Poly F., Lepeuple A.-S. and Fanlo J.-L. 2012a "Bacterial dynamics in steady-state biofilters: beyond functional stability." *FEMS Microbiol. Ecol.* 79 (1): 260-271.

Cabrol L., Malhautier L., Poly F., Lepeuple A.S. and Fanlo J.L. 2012b "Bacterial dynamics in steady-state biofilters: beyond functional stability." *FEMS Microbiol. Ecol.* 79 (1): 260-271.

Carberry J.J. 1964 "Designing laboratory catalytic reactors." *Ind. Eng. Chem.* 56 (11): 39-46.

511 Cárdenas-González B., Ergas S.J. and Switzenbaum M.S. 1999 "Characterization of compost
512 biofiltration media." *J. Air Waste Manag. Assoc.* 49 (7): 784-793.
513
514 Chang K. and Lu C. 2003 "Biofiltration of toluene and acetone mixutres by a trickle-bed air
515 biofilter." *World J. Microbiol. Biotechnol.* 19: 8.
516
517 Chen R., Liao Q., Tian X., Wang Y.Z., Zhu X. and Miao J.H. 2012 "Characterization of the
518 start-up behavior and steady-state performance of biotrickling filter removing low
519 concentration toluene waste gas." *Sci. China Technol. Sc.* 55 (6): 1701-1710.
520
521 Chen Y.S., Lin F.Y., Lin C.C., Tai C.Y.D. and Liu H.S. 2006 "Packing characteristics for
522 mass transfer in a rotating packed bed." *Ind. Eng. Chem. Res.* 45 (20): 6846-6853.
523
524 Cooper A.R. and Jeffreys G.V. 1971. *Chemical kinetics and reactor design,* Edinburgh,
525 Oliver & Boyd.
526
527 Cox H.H.J. and Deshusses M.A. 1999 "Biomass control in waste air biotrickling filters by
528 protozoan predation." *Biotechnol. Bioeng.* 62 (2): 216-224.
529
530 Cox H.H.J. and Deshusses M.A. 2002 "Co-treatment of H_2S and toluene in a biotrickling
531 filter." *Chem. Eng. J.* 87 (1): 101-110.
532
533 Cox H.H.J., Nguyen T.T. and Deshusses M.A. Elimination of toluene vapors in biotrickling
534 filters:performance and carbon balances. Annual Meeting and Exhibition of the Air
535 and Waste Management Association, 1998 San Diego,CA. AWMA,Pittsburgh,PA,
536 15.
537
538 Cox H.H.J., Nguyen T.T. and Deshusses M.A. 2000 "Toluene degradation in the recycle
539 liquid of biotrickling filters for air pollution control." *Appl. Microbiol. Biotechnol.* 54
540 (1): 133-137.
541
542 Dedysh S. and Dunfield P. 2014. Cultivation of methanotrophs. *In:* Mcgenity, TJ, Timmis,
543 KN & Fernandez, BN (eds.) *Hydrocarbon and Lipid Microbiology Protocols.*
544 Springer-Verlag.
545
546 Detchanamurthy S. and Gostomski P.A. 2013 "Development of a modified differential
547 biofiltration reactor with online sample and carbon dioxide monitoring system." *Asia-*
548 *Pac. J. Chem. Eng.* 8 (3): 414-424.
549
550 Giordano C., Spennati F., Mori G., Munz G. and Vannini C. 2018 "The microbial community
551 in a moving bed biotrickling filter operated to remove hydrogen sulfide from gas
552 streams." *Syst. Appl. Microbiol.* 41 (4): 399-407.
553
554 Goto S. and Smith J.M. 1975 "Trickle-bed reactor performance. Part i. Holdup and mass
555 transfer effects." *AIChE J.* 21 (4): 706-713.

He Z., Zhou L., Li G., Zeng X., An T., Sheng G., Fu J. and Bai Z. 2009 "Comparative study of the eliminating of waste gas containing toluene in twin biotrickling filters packed with molecular sieve and polyurethane foam." *J. Hazard. Mater.* 167 (1–3): 275-281.

Hwang S.J. and Tang H.M. 1997 "Kinetic behavior of the toluene biofiltration process." *J. Air Waste Manag. Assoc.* 47 (6): 664-673.

Jiménez L., Arriaga S. and Aizpuru A. 2016 "Assessing biofiltration repeatability: Statistical comparison of two identical toluene removal systems." *Environ. Technol.* 37 (6): 681-693.

Jorio H., Bibeau L. and Heitz M. 2000 "Biofiltration of air contaminated by styrene: Effect of nitrogen supply, gas flow rate, and inlet concentration." *Environ. Sci. Technol.* 34 (9): 1764-1771.

Kim S. and Deshusses M.A. 2005 "Understanding the limits of H_2S degrading biotrickling filters using a differential biotrickling filter." *Chem. Eng. J.* 113 (2-3): 119-126.

Kim S. and Deshusses M.A. 2008 "Determination of mass transfer coefficients for packing materials used in biofilters and biotrickling filters for air pollution control. 1. Experimental results." *Chem. Eng. Sci.* 63 (4): 841-855.

Krailas S., Pham Q.T., Amal R., Jiang J.K. and Heitz M. 2000 "Effect of inlet mass loading, water and total bacteria count on methanol elimination using upward flow and downward flow biofilters." *J. Chem. Technol. Biotechnol.* 75 (4): 299-305.

Kumar M., Giri B.S., Kim K.-H., Singh R.P., Rene E.R., López M.E., Rai B.N., Singh H., Prasad D. and Singh R.S. 2019 "Performance of a biofilter with compost and activated carbon based packing material for gas-phase toluene removal under extremely high loading rates." *Bioresour. Technol.* 285: 121317.

Lebrero R., Estrada J.M., Munoz R. and Quijano G. 2012 "Toluene mass transfer characterization in a biotrickling filter." *Biochem. Eng. J.* 60: 44-49.

Lepeuple A.-S., Cabrol L., Fanlo J.-L., Malhautier L. and Poly F. 2012 "Bacterial dynamics in steady-state biofilters: beyond functional stability." *FEMS Microbiol. Ecol.* 79 (1): 260-271.

Li G.Y., He Z., An T.C., Zeng X.Y., Sheng G.Y. and Fu J. 2008 "Comparative study of the elimination of toluene vapours in twin biotrickling filters using two microorganisms *Bacillus cereus* S1 and S2." *J. Chem. Technol. Biotechnol.* 83 (7): 1019-1026.

599 Liu D.Z., Andreasen R.R., Poulsen T.G. and Feilberg A. 2015 "A comparative study of mass
600 transfer coefficients of reduced volatile sulfur compounds for biotrickling filter
601 packing materials." *Chem. Eng. J.* 260: 209-221.
602
603 López de León L.R., Deaton K.E. and Deshusses M.A. 2019 "Miniaturized biotrickling filters
604 and capillary microbioreactors for process intensification of voc treatment with
605 intended application to indoor air." *Environ. Sci. Technol.* 53 (3): 1518-1526.
606
607 López M.E., Rene E.R., Malhautier L., Rocher J., Bayle S., Veiga M.C. and Kennes C. 2013
608 "One-stage biotrickling filter for the removal of a mixture of volatile pollutants from
609 air: Performance and microbial community analysis." *Bioresour. Technol.* 138: 245-
610 252.
611
612 Maiti R.N., Sen P.K. and Nigam K.D.P. 2004 "Trickle-bed reactors: Liquid distribution and
613 flow texture." *Rev. Chem. Eng.* 20 (1-2): 57-109.
614
615 McKelvey J.M. and Hoelscher H.E. 1957 "Apparatus for preparation of very dilute gas
616 mixtures." *Anal. Chem.* 29 (1): 123-123.
617
618 Mederos F.S., Ancheyta J. and Chen J.W. 2009 "Review on criteria to ensure ideal behaviors
619 in trickle-bed reactors." *Appl. Catal. A-Gen.* 355 (1-2): 1-19.
620
621 Mirpuri R., Jones W. and Bryers J.D. 1997 "Toluene degradation kinetics for planktonic and
622 biofilm-grown cells of *Pseudomonas putida* 54G." *Biotechnol. Bioeng.* 53 (6): 535-
623 546.
624
625 Misiaczek O., Paca J., Halecky M., Gerrard A.M., Sobotka M. and Soccol C.R. 2007 "Start-
626 up and performance characteristics of a trickle bed reactor degrading toluene." *Braz.*
627 *Arch. Biol. Technol.* 50 (5): 871-877.
628
629 Mohammed I., Bauer T., Schubert M. and Lange R. 2015 "Gas-liquid distribution in tubular
630 reactors with solid foam packings." *Chem. Eng. Process.* 88: 10-18.
631
632 Nelson G.O. 1971. *Controlled test atmospheres; principles and techniques,* Ann
633 Arbor,Michigan, Ann Arbor Science.
634
635 Ottengraf S.P.P. and Vandenoever A.H.C. 1983 "Kinetics of organic-compound removal
636 from waste gases with a biological filter." *Biotechnol. Bioeng.* 25 (12): 3089-3102.
637
638 Perez J., Montesinos J.L. and Godia F. 2006 "Gas-liquid mass transfer in an up-flow
639 cocurrent packed-bed biofilm reactor." *Biochem. Eng. J.* 31 (3): 188-196.
640
641 Ranasinghe M.A. and Gostomski P.A. 2003 "A novel reactor for exploring the effect of water
642 content on biofilter degradation rates." *Environ. Prog.* 22 (2): 103-109.
643

644 Rene E.R., Murthy D.V.S. and Swaminathan T. 2005 "Performance evaluation of a compost
645 biofilter treating toluene vapours." *Process Biochem.* 40 (8): 2771-2779.
646
647 Rocha-Rios J., Kraakman N.J.R., Kleerebezem R., Revah S., Kreutzer M.T. and van
648 Loosdrecht M.C.M. 2013 "A capillary bioreactor to increase methane transfer and
649 oxidation through Taylor flow formation and transfer vector addition." *Chem. Eng. J.*
650 217: 91-98.
651
652 Ryu H.W., Cho K.S. and Chung D.J. 2010 "Relationships between biomass, pressure drop,
653 and performance in a polyurethane biofilter." *Bioresour. Technol.* 101 (6): 1745-
654 1751.
655
656 Ryu H.W., Kim S.J., Cho K.S. and Lee T.H. 2008 "Toluene degradation in a polyurethane
657 biofilter at high loading." *Biotechnol. Bioprocess Eng.* 13 (3): 360-365.
658
659 San-Valero P., Penya-Roja J.M., Alvarez-Hornos F.J. and Gabaldon C. 2014 "Modelling
660 mass transfer properties in a biotrickling filter for the removal of isopropanol." *Chem.*
661 *Eng. Sci.* 108: 47-56.
662
663 Sander R. 2015 "Compilation of Henry's law constants (version 4.0) for water as solvent."
664 *Atmos. Chem. Phys.* 15 (8): 4399-4981.
665
666 Shen Y., Stehmeier L.G. and Voordouw G. 1998 "Identification of hydrocarbon-degrading
667 bacteria in soil by reverse sample genome probing." *Appl. Environ. Microbiol.* 64 (2):
668 637-45.
669
670 Shukla A.K., Singh R.S., Upadhyay S.N. and Dubey S.K. 2011 "Substrate inhibition during
671 bio-filtration of TCE using diazotrophic bacterial community." *Bioresour. Technol.*
672 102 (3): 3561-3563.
673
674 Singh R.S., Rai B.N. and Upadhyay S.N. 2010 "Removal of toluene vapour from air stream
675 using a biofilter packed with polyurethane foam." *Process Saf. Environ. Prot.* 88 (5):
676 366-371.
677
678 Song J.H. and Kinney K.A. 2000 "Effect of vapor-phase bioreactor operation on biomass
679 accumulation, distribution, and activity: Linking biofilm properties to bioreactor
680 performance." *Biotechnol. Bioeng.* 68 (5): 508-516.
681
682 Sun D.F., Li J.J., Xu M.Y., An T.C., Sun G.P. and Guo J. 2013 "Toluene removal efficiency,
683 process robustness, and bacterial diversity of a biotrickling filter inoculated with
684 *Burkholderia sp* Strain T3." *Biotechnol. Bioprocess Eng.* 18 (1): 125-134.
685
686 Thapa C., Shakya P., Shrestha R., Pal S. and Manandhar P. 2019 "Isolation of
687 polyhydroxybutyrate (PHB) producing bacteria, optimization of culture conditions

for PHB production, extraction and characterization of PHB." *Nepal J. Biotechnol.* 6: 62-68.

Tsuneda S., Aikawa H., Hayashi H., Yuasa A. and Hirata A. 2003 "Extracellular polymeric substances responsible for bacterial adhesion onto solid surface." *FEMS Microbiol. Lett.* 223 (2): 287-292.

Wang L., Yang C., Cheng Y., Huang J., Yang H., Zeng G., Lu L. and He S. 2014 "Enhanced removal of ethylbenzene from gas streams in biotrickling filters by Tween-20 and Zn(II)." *J. Environ. Sci-China* 26 (12): 2500-2507.

Wang Y.F., Mao Z.S. and Chen J.Y. 1998 "Scale and variance of radial liquid maldistribution in trickle beds." *Chem. Eng. Sci.* 53 (6): 1153-1162.

Weber F.J. and Hartmans S. 1996 "Prevention of clogging in a biological trickle-bed reactor removing toluene from contaminated air." *Biotechnol. Bioeng.* 50 (1): 91-97.

Zilli M., Palazzi E., Sene L., Converti A. and Del Borghi M. 2001 "Toluene and styrene removal from air in biofilters." *Process Biochem.* 37 (4): 423-429.

720

721

722

723

724

725

Table 1. Operating conditions of toluene-degrading BTFs reported in the literature

Reference	Gas/Liq. Flow	Packing material	EC_{max} ($g/m^3\ h^1$)	C_0 (g/m^3)	V_g (m/h^1)	V_l (m/h^1)	V_g/V_l
(Misiaczek et al. 2007)	counter-current	PP[a] high flow rings	11	0.1	272	2.32	117
(Weber and Hartmans 1996)	counter current	Pall rings[c]	30	0.7	99	7.10	14
(Cox et al. 1998)	cocurrent	PP[a] Pall rings	40	2.0	83	8.0	10
(Chen et al. 2012)	both modes	ceramic spheres	50	0.6	7.0	0.34	21
(Cox and Deshusses 2002)	cocurrent	PP[a] Pall rings	70	2.3	658	5.60	117
(Cox and Deshusses 1999)	cocurrent	PP[a] Pall rings	83	1.0	83	10.0	8
(Singh et al. 2010)	cocurrent	PUF	90	2.5	35	--	--
(Chang and Lu 2003)	cocurrent	coal particles	113	3.0	34.0	0.02	1700
(Lebrero et al. 2012)	counter-current	PUF[b]	180	5.0	57-260	0.60	95 – 433
(Sun et al. 2013)	counter current	ceramisite	234	2.1	0.9	0.001	900
(Zilli et al. 2001)	counter current	peat and glass beads	242	2.0	17.8	--	--
(Li et al. 2008)	cocurrent	ceramic particles	300	8.0	20	0.01	2,000
(He et al. 2009)	cocurrent	molecular sieve	373	9.0	13	0.07	186
(Ryu et al. 2008)	counter current	PUF	3,700	3.6	1,972	0.012	164,300
(Kumar et al. 2019)	counter current	compost and AC[d]	6,665	37.4	93	0.002	46,500

[a] PP - polypropylene

[b] PUF – polyurethane foam

[c] material not indicated

[d] activated carbon

LIST OF FIGURES

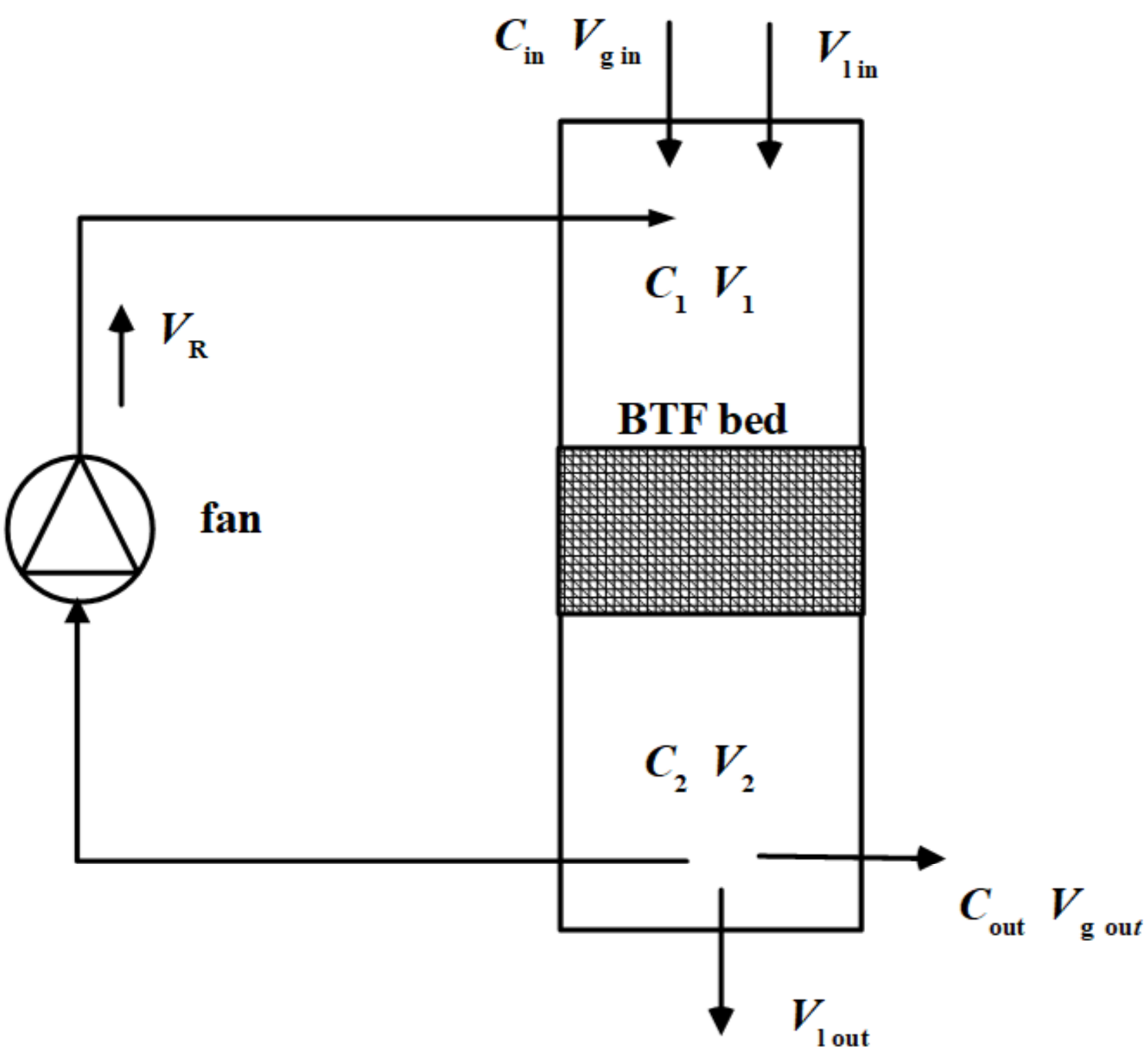
C_{in} $V_{g\,in}$
$V_{l\,in}$
C_1 V_1
V_R
BTF bed
fan
C_2 V_2
C_{out} $V_{g\,out}$
$V_{l\,out}$


external nutrient reservoir
reactor bed
fan
fan speed controller
aerosol generator

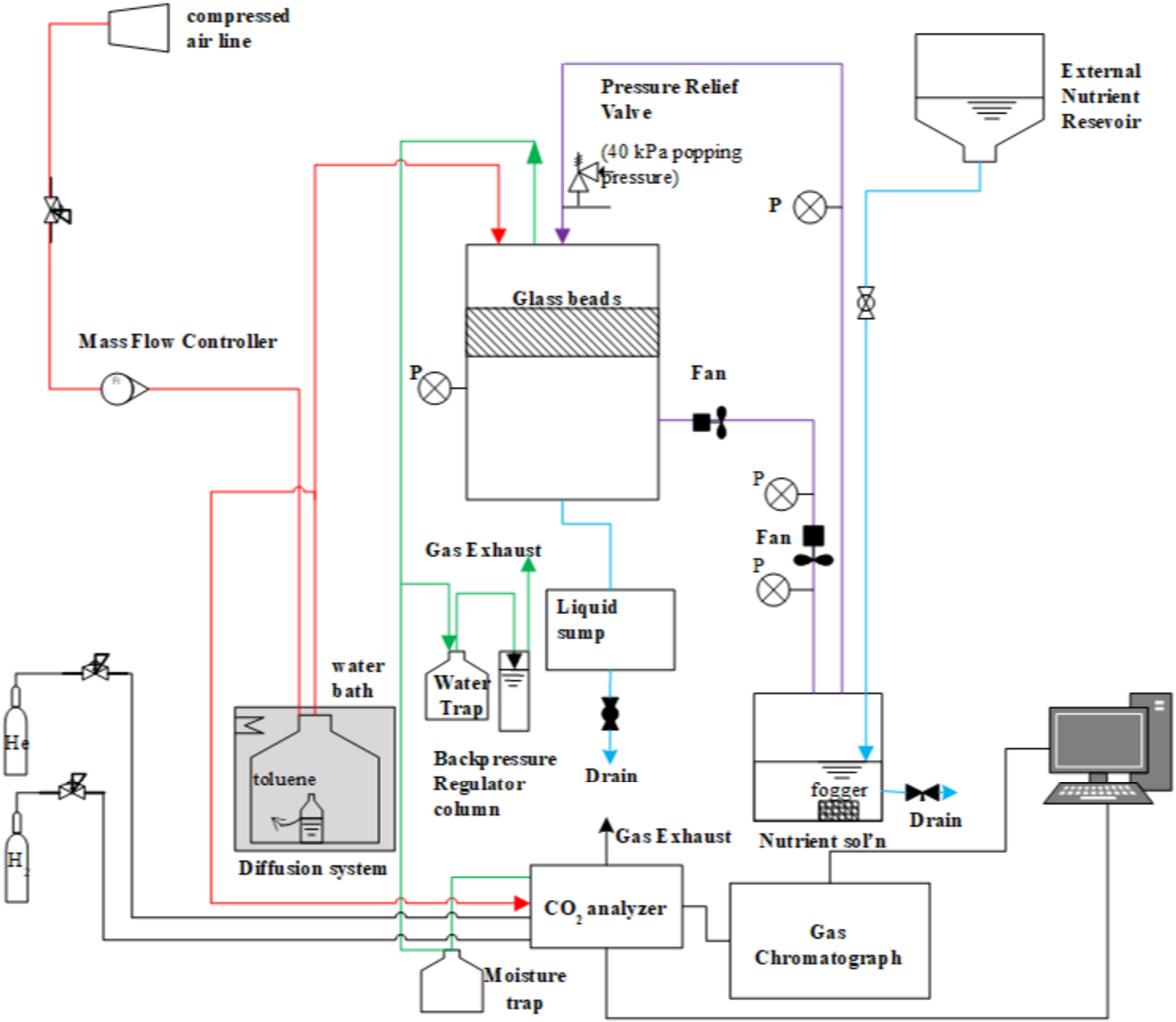
compressed air line
Pressure Relief Valve
(40 kPa popping pressure)
External Nutrient Resevoir
P
Glass beads
Mass Flow Controller
P
Fan
P
Fan
P
Gas Exhaust
Liquid sump
water bath
Water Trap
He
toluene
Backpressure Regulator column
Drain
fogger
Drain
Nutrient sol'n
Gas Exhaust
H_2
Diffusion system
CO_2 analyzer
Gas Chromatograph
Moisture trap

A

day 3 day 15 day 25

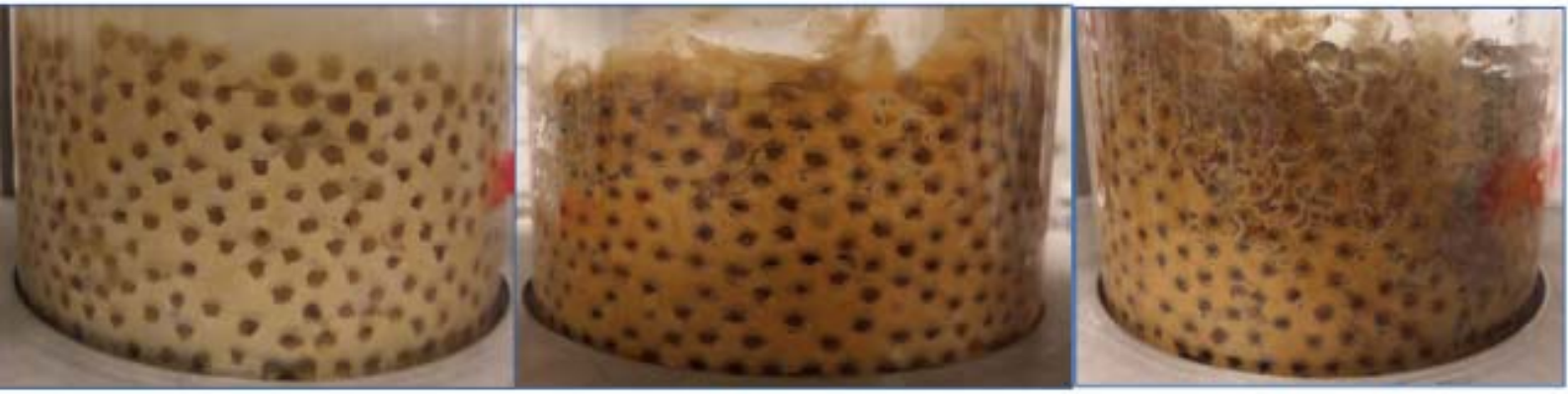

day 35 day 60 day 85

B

cross-section of the DBTF bed with biofilm (day 31)

day 24 day 37 day 45 day 81

A

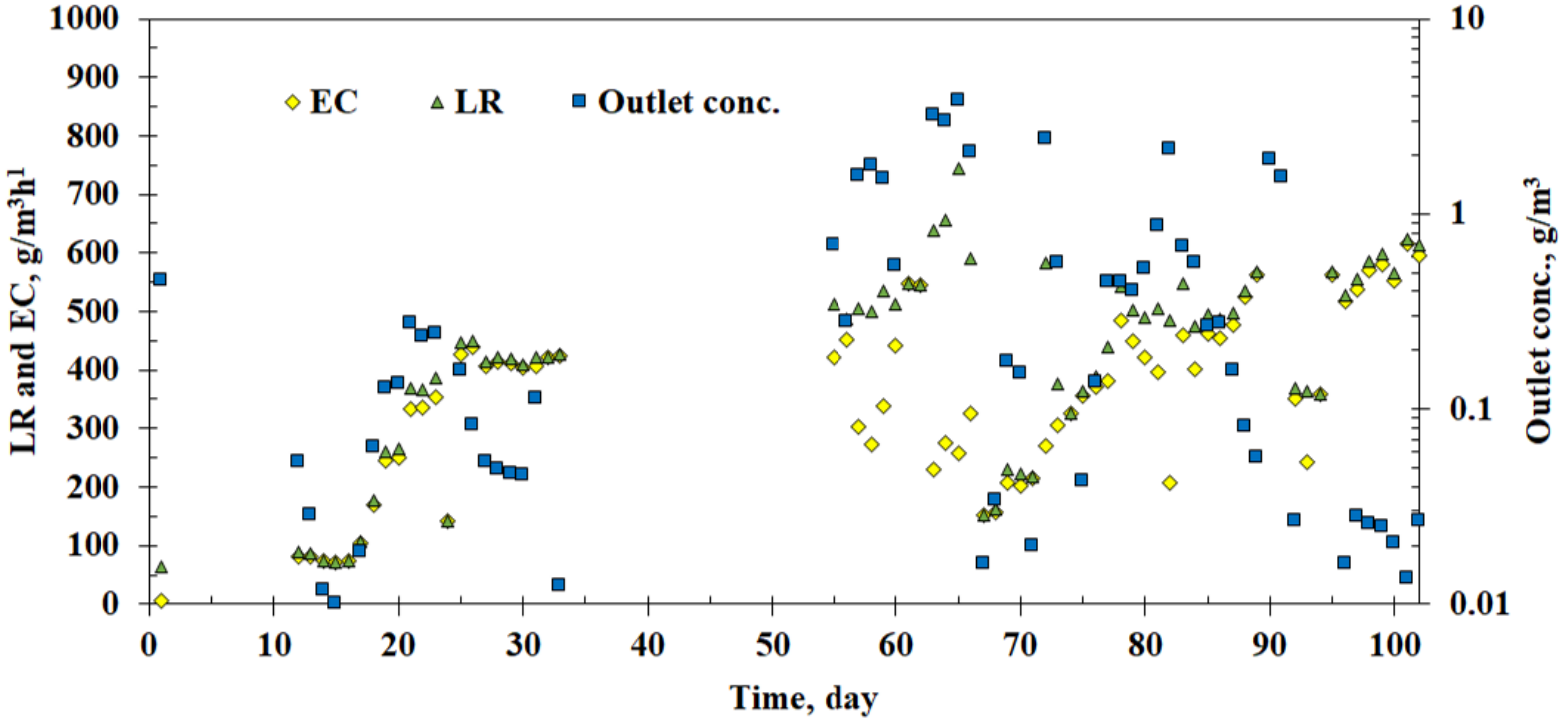
EC
LR
Outlet conc.
LR and EC, g/m³h¹
Outlet conc., g/m³
Time, day

B

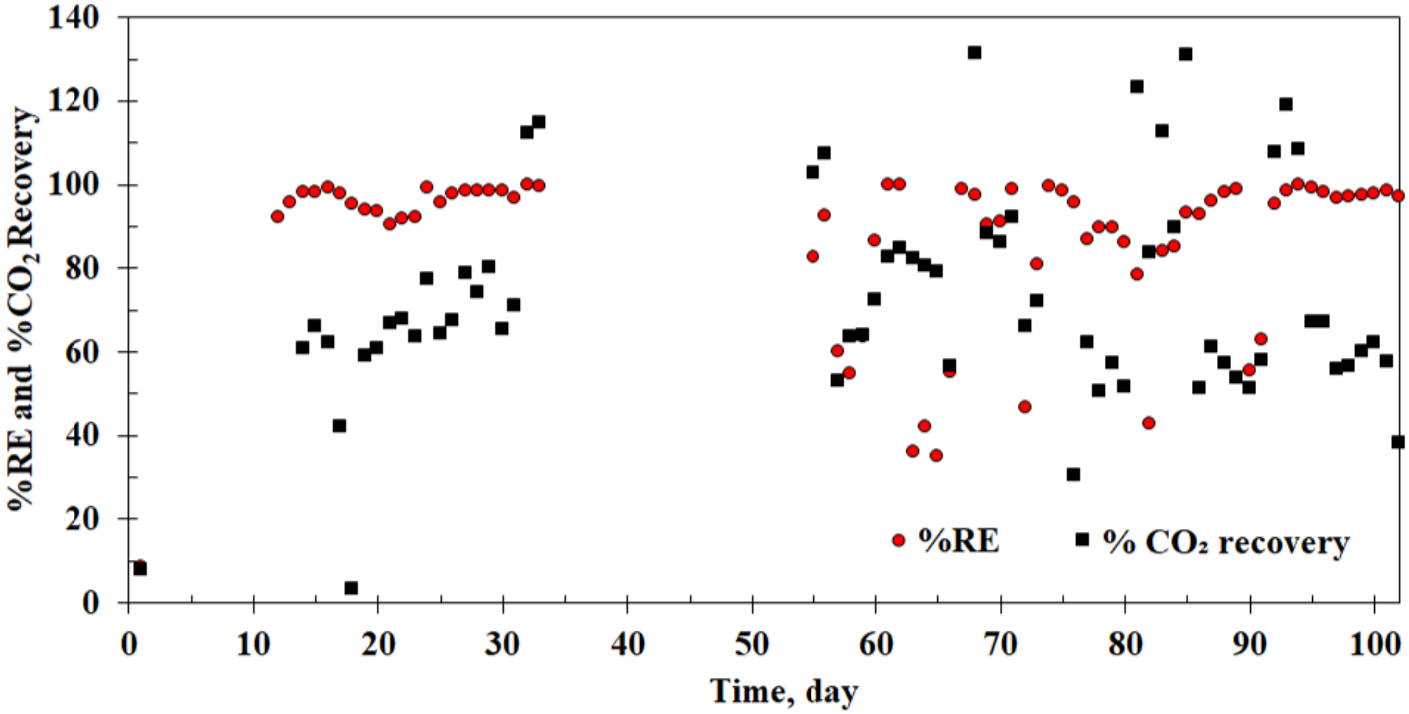
%RE
% CO₂ recovery
%RE and %CO₂ Recovery
Time, day

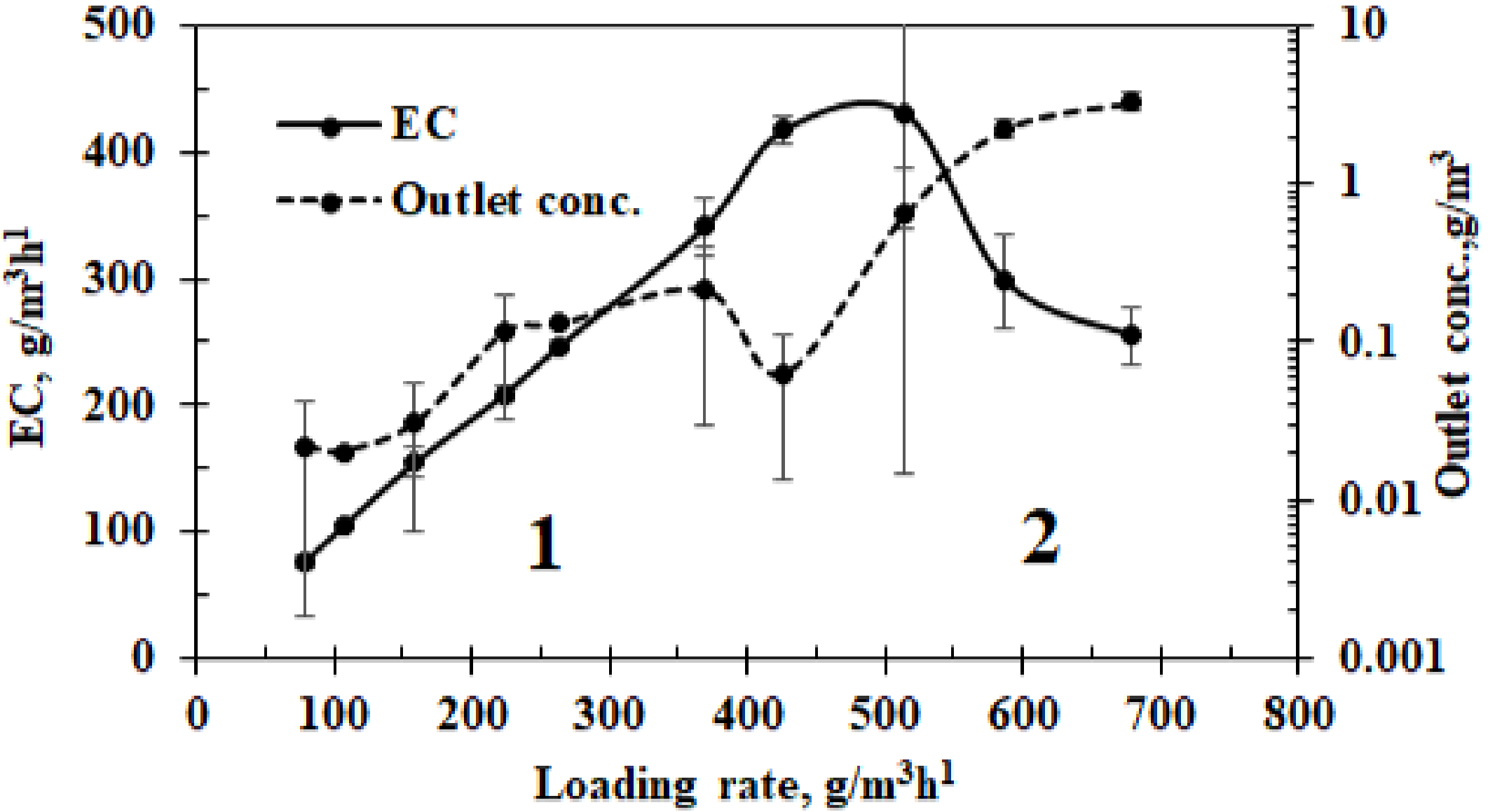
EC
Outlet conc.
1
2
EC, g/m3h1
Outlet conc., g/m3
Loading rate, g/m3h1
500
400
300
200
100
0
10
1
0.1
0.01
0.001
0
100
200
300
400
500
600
700
800

Supplemental information 1

Estimation of recycle rate and concentration gradient across the bed

A. Given:

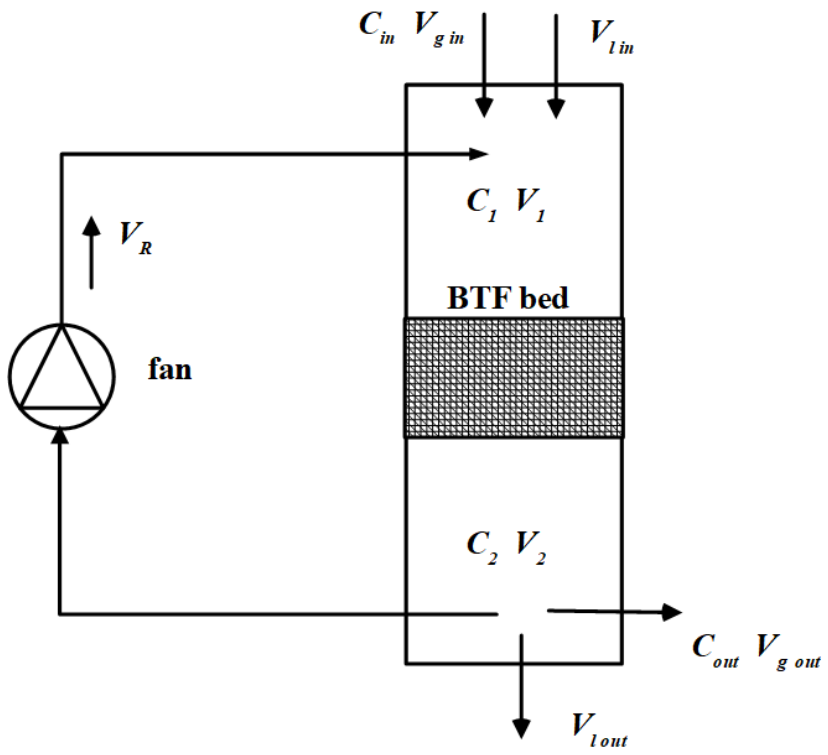

Figure S1. Schematic diagram showing the gas flow in a recycle reactor.

where:

C_{in} = toluene concentration of the inlet feed, $g \cdot m^{-3}$

V_{in} = volumetric flow rate of the inlet feed, $m^3 \cdot h^{-1}$

C_1 = toluene concentration at the headspace, $g \cdot m^{-3}$

V_1 = volumetric flow rate entering the bed, $m^3 \cdot h^{-1}$

C_2 = toluene concentration exiting the bed, $g \cdot m^{-3}$

V_2 = volumetric flow rate exiting the bed, $m^3 \cdot h^{-1}$

V_R = gas recycle rate, $m^3 \cdot h^{-1}$

C_{out} = toluene concentration of the outlet gas, $g \cdot m^{-3}$

V_{out} = volumetric flow rate of the outlet gas, $m^3 \cdot h^{-1}$

$V_{L\ in}$ = volumetric flow rate of the incoming liquid phase, $m^3 \cdot h^{-1}$

$V_{L\ out}$ = volumetric flow rate of the outgoing liquid phase, $m^3 \cdot h^{-1}$

Denote: V_B = volume of the bed, m^3

X_s = single pass conversion, %

X_o = overall conversion, %

R_R = recycle ratio, unitless

B. Assumptions:

Q = 0.00084 $m^3 \cdot min^{-1}$ (from 840 $mL \cdot min^{-1}$)

C_0 = 1 $g \cdot m^{-3}$

EC = 80 $g \cdot m^{-3}\ h^{-1}$ (from Appendix 4.1)

V_B = 0.0003925 m^3 (based on a bed thickness of 50 mm and bed diameter of 100 mm)

C. Derivation of relevant equations:

$$R_R = \frac{V_R}{V_{in}} \quad (1)$$

At point 1 in the reactor, $V_1 = V_{in} + V_R$;

Expressing V_R in terms of R_R and V_{in}; $V_1 = V_0 + R_R V_{in}$; (2)

$V_1 = V_0 (1 + R_R)$ (3)

Calculating for overall conversion, X_o;

$$X_0 = \frac{\dot{V}_0 - \dot{V}_2}{\dot{V}_0} \quad (4)$$

where $\dot{W}_0$ = mass loading of toluene per unit time at the entrance of the reactor, g·h^{-1}

$\dot{W}_2$ = amount of toluene passing through at point 2 (below the bed) per unit time, g·h^{-1}

Expressing $\dot{W}_2$ in terms of $\dot{W}_0$ and X_0;

$$\dot{W}_2 = \dot{W}_0 - \dot{W}_0 X_0 \tag{5}$$

Calculating for single pass conversion, X_s;

$$X_s = \frac{\dot{W}_1 - \dot{W}_2}{\dot{W}_1} \tag{6}$$

where $\dot{W}_1$ = amount of toluene passing through at point 1 (at the headspace of the reactor) per unit time, g·h^{-1}

Recall that variables in Eqn. 2 can be expressed in terms of the amount of toluene passing per unit time, hence $\dot{W}_1 = \dot{W}_0 + R_R \dot{W}_2$.

It should also be noted that at point 2, $\dot{W}_2 = \dot{W}_0 + \dot{W}_2 R_R$;

Since single pass conversion is assumed to be minimal, $\dot{W}_2 = \dot{W}_0$, hence $\dot{W}_2 = \dot{W}_2(1 + R_R)$.

Substituting the above relationships to Eqn. 6,

$$X_s = \frac{\left(\dot{W}_0 + R_R \dot{W}_2\right) - \left[\dot{W}_2(1 + R_R)\right]}{\dot{W}_0 + R_R \dot{W}_2}$$

$$X_s = \frac{\dot{W}_0 + R_R \dot{W}_2 - \dot{W}_2 - R_R \dot{W}_2}{\dot{W}_0 + R_R \dot{W}_2}$$

$$X_s = \frac{\dot{W}_0 - \dot{W}_2}{\dot{W}_0 + R_R \dot{W}_2} \tag{7}$$

Substituting Eqn. 5 to Eqn. 7;

$$X_s = \frac{\dot{V}_0 - \left(\dot{V}_0 - \dot{V}_0 X_0\right)}{\dot{V}_0 + \left[R_R\left(\dot{V}_0 - \dot{V}_0 X_0\right)\right]}$$

$$X_s = \frac{\dot{V}_0 - \dot{V}_0 + \dot{V}_0 X_0}{\dot{V}_0 + \dot{V}_0 R_R - R_R \dot{V}_0 X_0}$$

$$X_s = \frac{\dot{V}_0 X_0}{\dot{V}_0 (1 + R_R - R_R X_0)}$$

$$X_s = \frac{X_0}{\left(1 + R_R - R_R X_0\right)}$$

$$X_s\left(1 + R_R - R_R X_0\right) = X_0$$

$$X_s + X_s R_R - X_s R_R X_0 = X_0$$

$$X_s + X_s R_R = X_0 + X_s R_R X_0$$

$$X_s\left(1 + R_R\right) = X_0\left(1 + X_s R_R\right)$$

$$X_0 = \frac{X_s\left(1 + R_R\right)}{1 + R_R X_s}$$

Expressing X_s in terms of X_0 and R_R;

$$1 + R_R X_s\left(X_0\right) = X_s\left(1 + R_R\right)$$

$$1 = X_s + X_s R_R + R_R X_s X_0$$

$$1 = X_s\left(1 + R_R + R_R X_0\right)$$

$$X_s = \frac{1}{1 + R_R + R_R X_0} \qquad (8)$$

Recall that when there is no gas recycling in the system (i.e. R_R is zero), hence

$$X_s = X_0 = \frac{EC * V_B}{V_0 * C_0} \quad (9)$$

Eqns. 8 and 9 were used in calculating the concentration gradient across the bed at varying recycling rate (Table S1).

Table S1. Estimated concentration gradient across the bed with varying recycle ratio.

Recycling Ratio	**Recycling Rate ($m^3 \cdot min^{-1}$)**	**Recycling Rate ($L \cdot min^{-1}$)**	**X_s (single pass conversion, %)**	**Conc. Gradient across the bed ($g \cdot m^{-3}$)**	**Conc. Gradient across the bed (ppm)**
60	0.050	50.40	1.02	0.01	2.70
55	0.046	46.20	1.11	0.01	2.94
50	0.042	42.00	1.22	0.01	3.23
45	0.038	37.80	1.35	0.01	3.58
40	0.034	33.60	1.52	0.02	4.03
35	0.029	29.40	1.73	0.02	4.59
30	0.025	25.20	2.01	0.02	5.34
25	0.021	21.00	2.41	0.02	6.38
20	0.017	16.80	2.99	0.03	7.93
15	0.013	12.60	3.95	0.04	10.47
10	0.008	8.40	5.80	0.06	15.40
7	0.006	5.88	8.09	0.08	21.47
6	0.005	5.04	9.31	0.09	24.71
5	0.004	4.20	10.97	0.11	29.11
4	0.003	3.36	13.35	0.13	35.42
3	0.003	2.52	17.04	0.17	45.21
2	0.002	1.68	23.55	0.24	62.50
1	0.001	0.84	38.12	0.38	101.17
0	0.000	0.00	62.30	1.00	165.32

Supplemental Information 2

Various graphs and images from the experiments

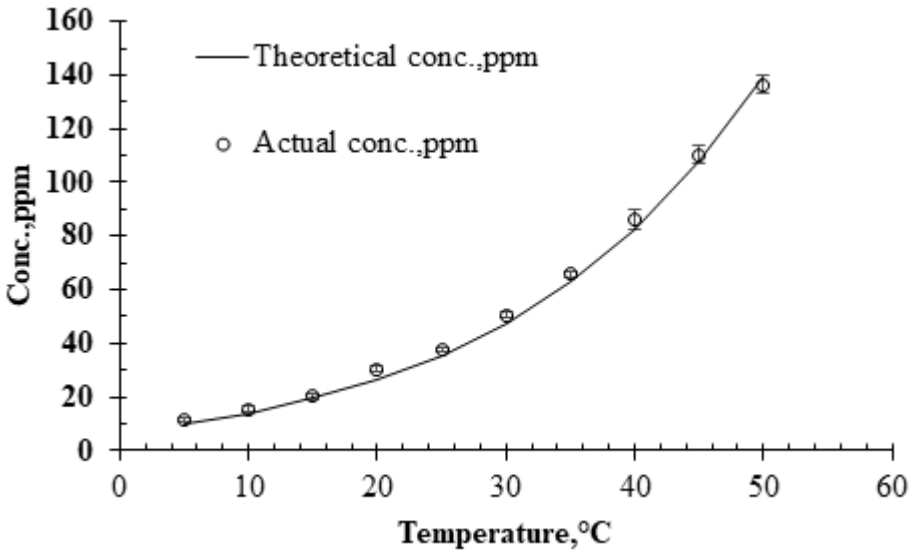

Figure S1. Actual conc.* vs. theoretical conc. generated by the diffusion system.

* Data for actual concentration at varying temperature are averages of at least 10 readings with <8% RSD.

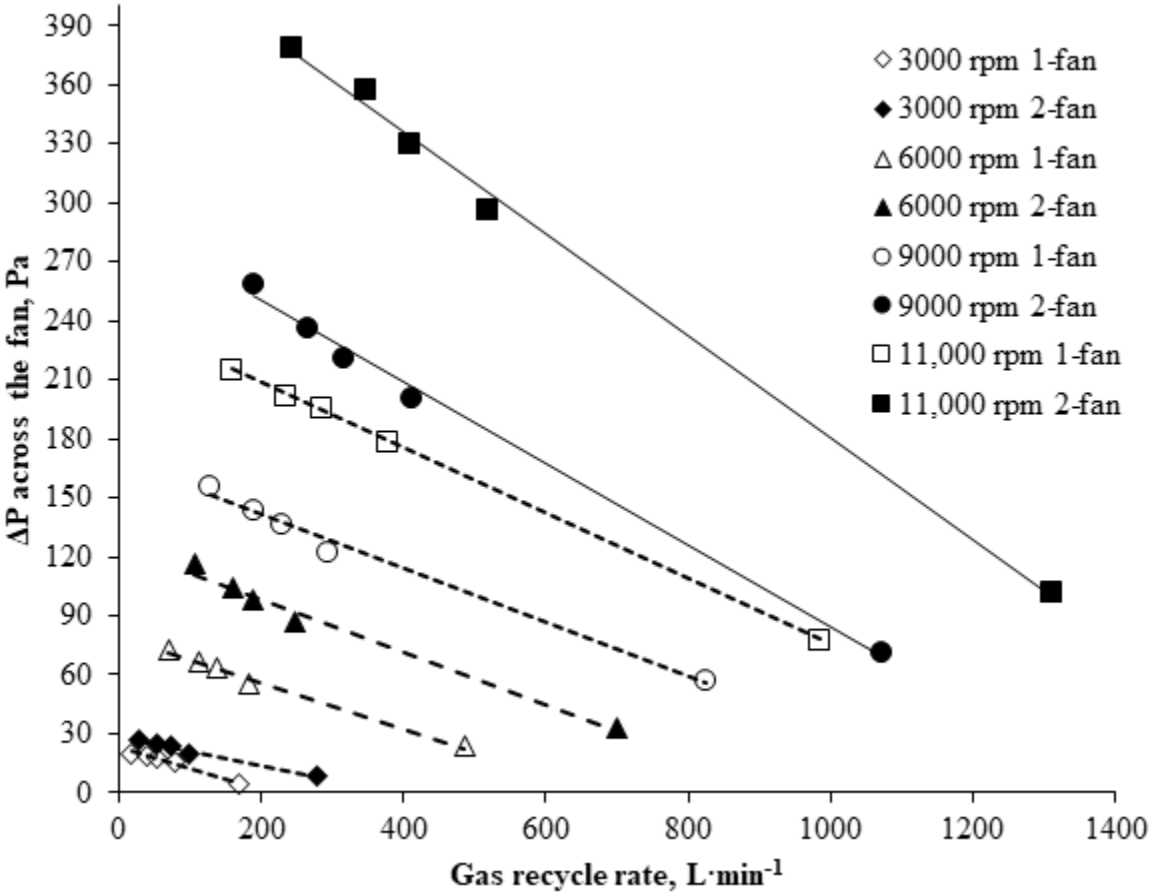

Figure S2. Fan performance curve at varying fan speed (single and dual fan in series-configuration).

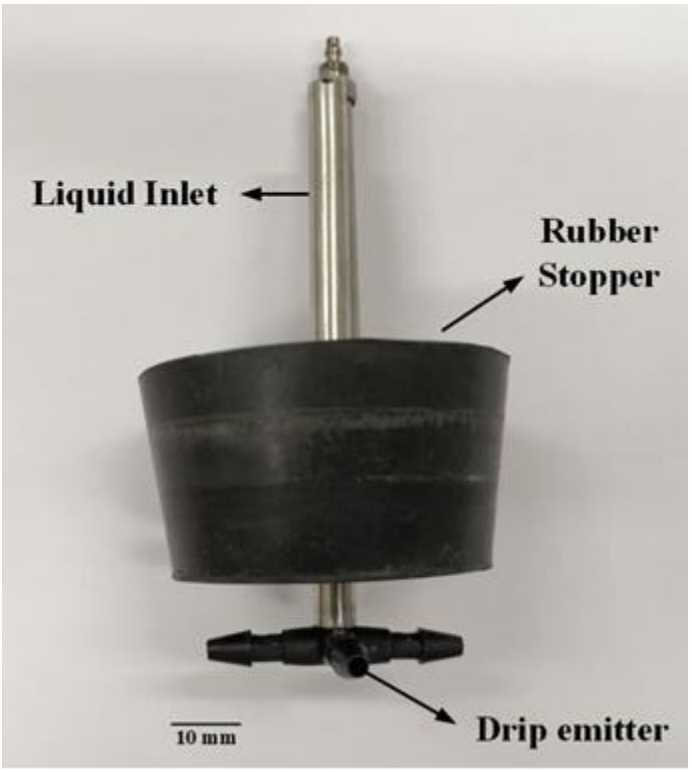

Figure S3. Four-port nozzle used in the column reactor.

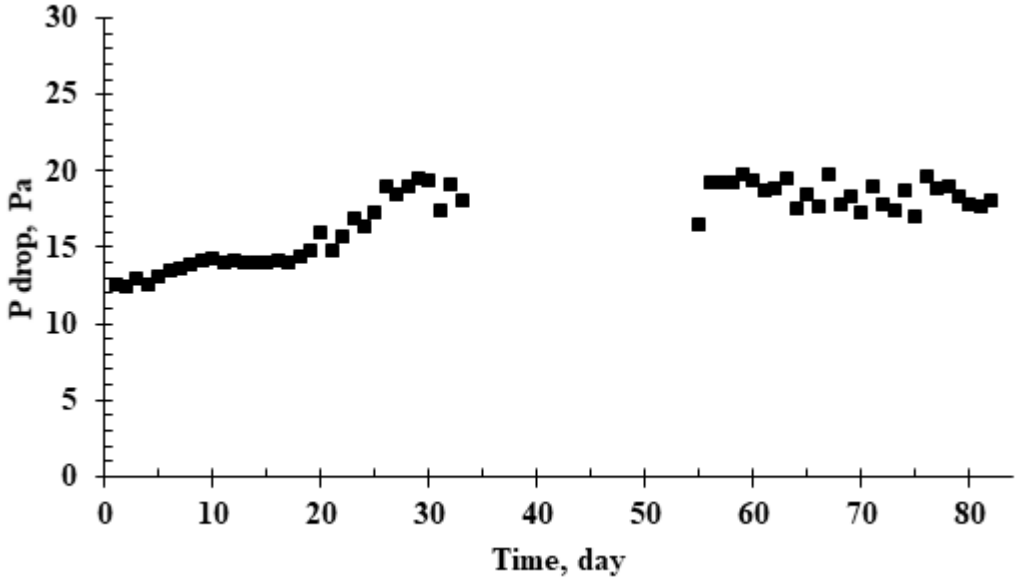

Figure S4. Pressure drop across the bed over the 80-day run at a fan speed of 3,000 rpm. Each pressure measurement is an average of 5 readings with <5% relative standard deviation (RSD).

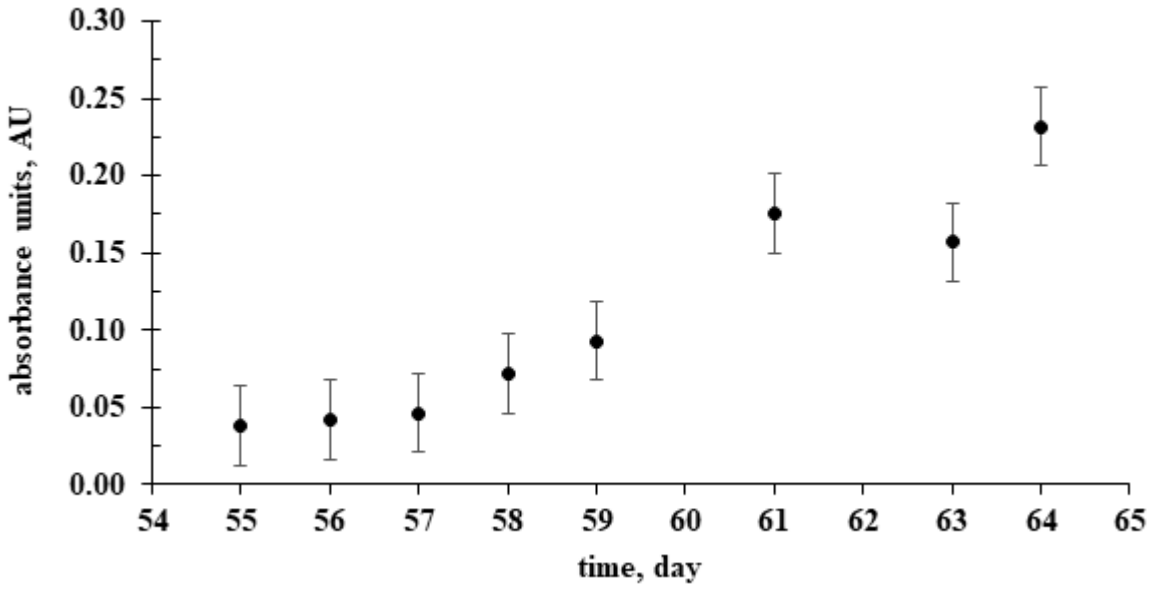

Figure S5. Change in the absorbance (at 600 nm) of the medium in the aerosol reservoir.

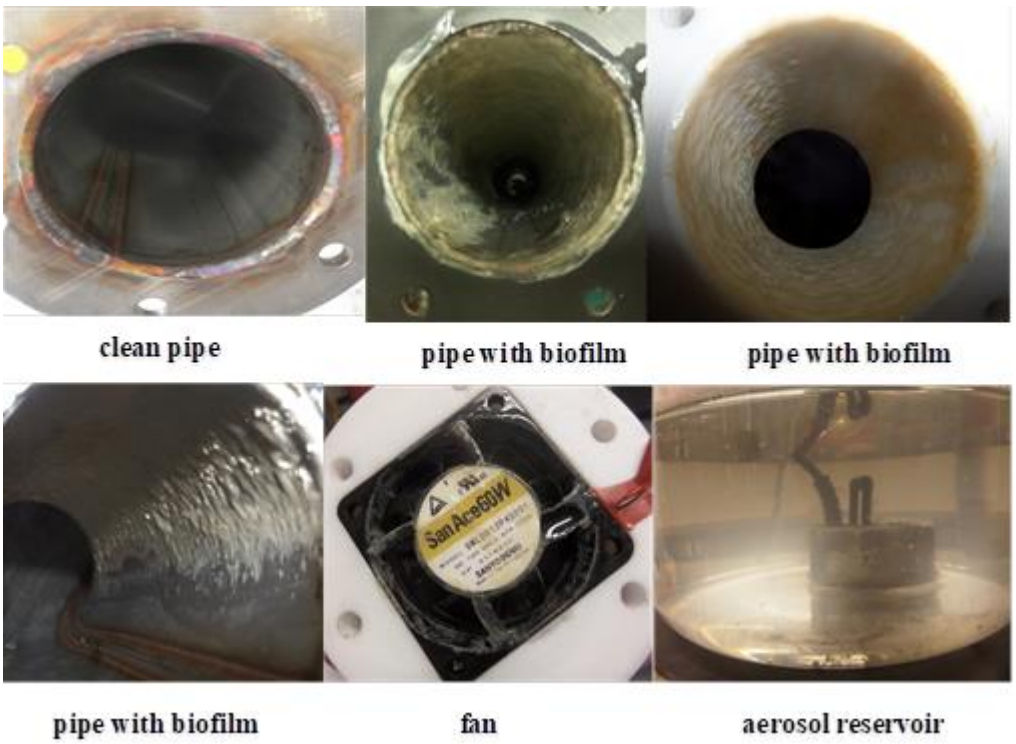

Figure S6. Biofilm development in the surfaces of the pipe, fan and suspended biomass in the aerosol reservoir.

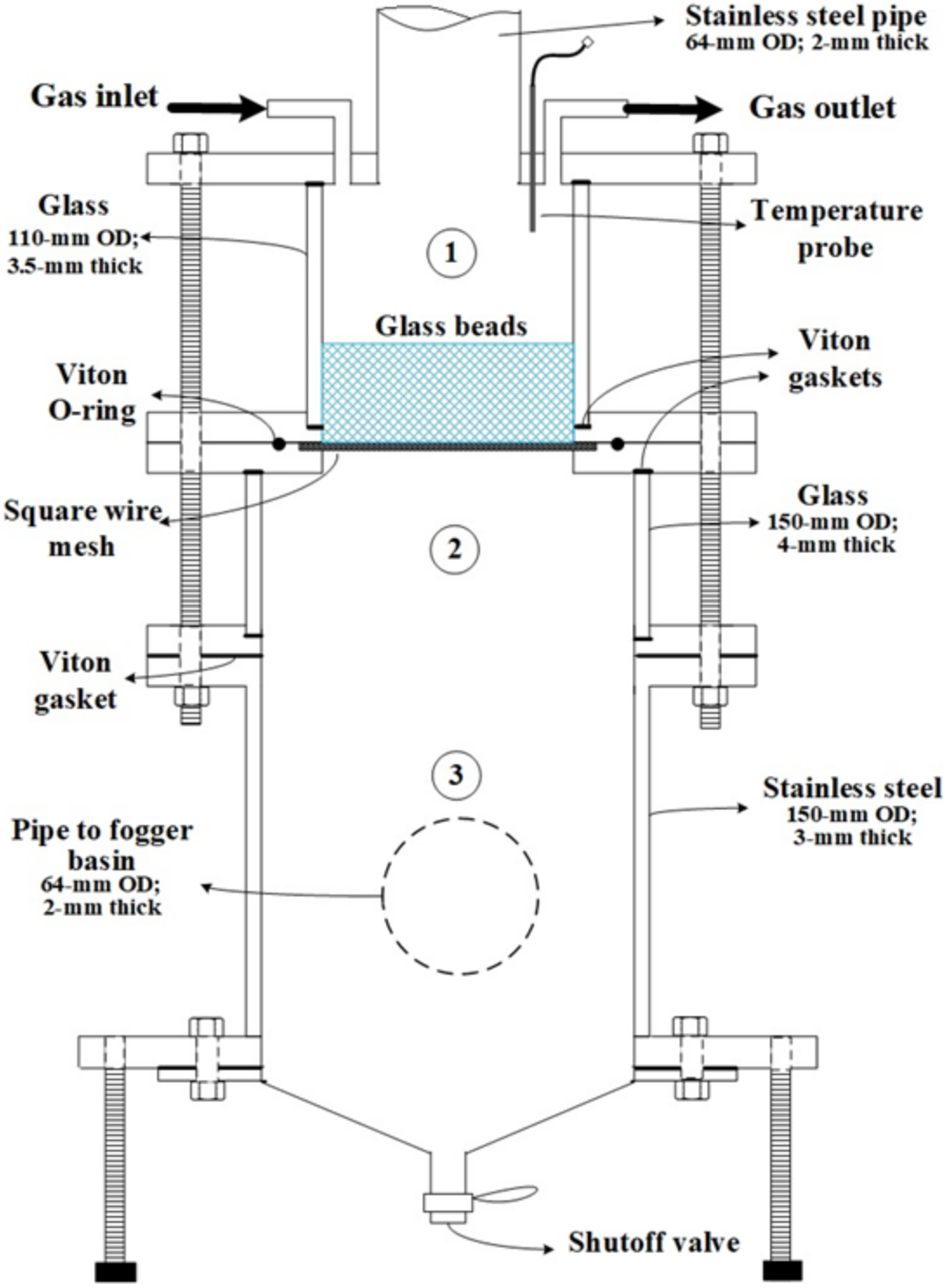

Figure S7. The three main sections of the differential BTF's reactor bed.

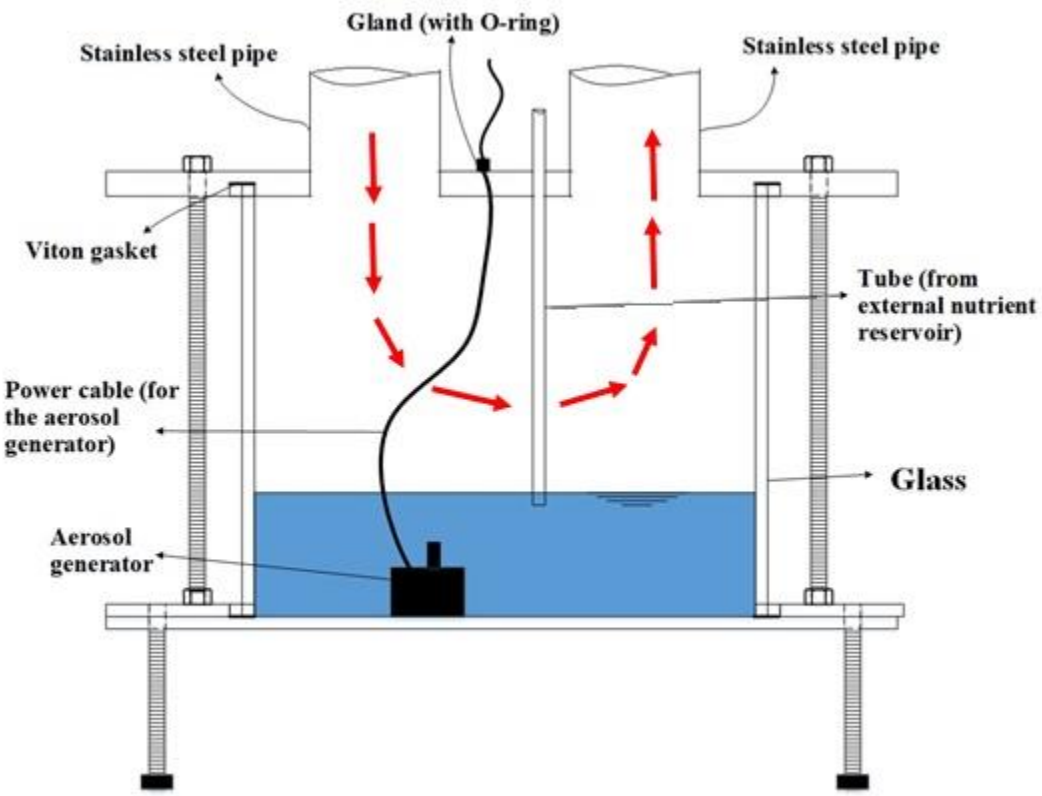

Figure S8. The aerosol reservoir of the differential BTF system. Red arrows indicate gas recycle.

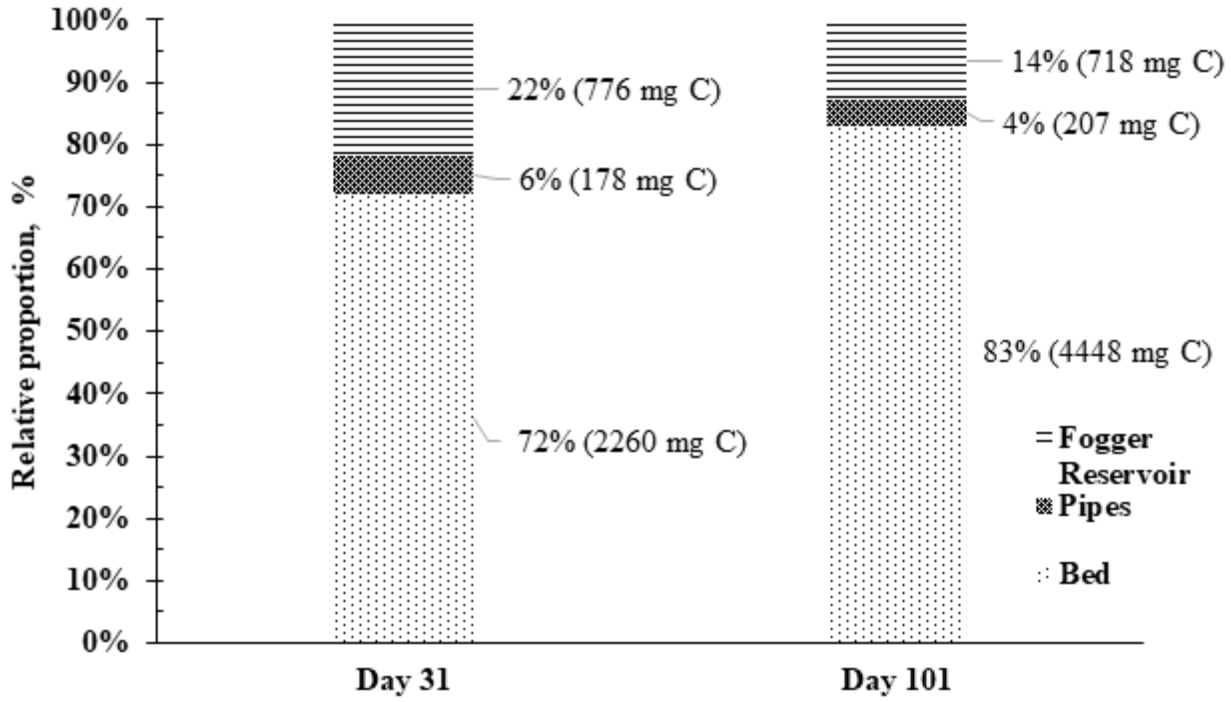

Figure S9. Relative proportion of organic carbon in each portion of the DBTF system.

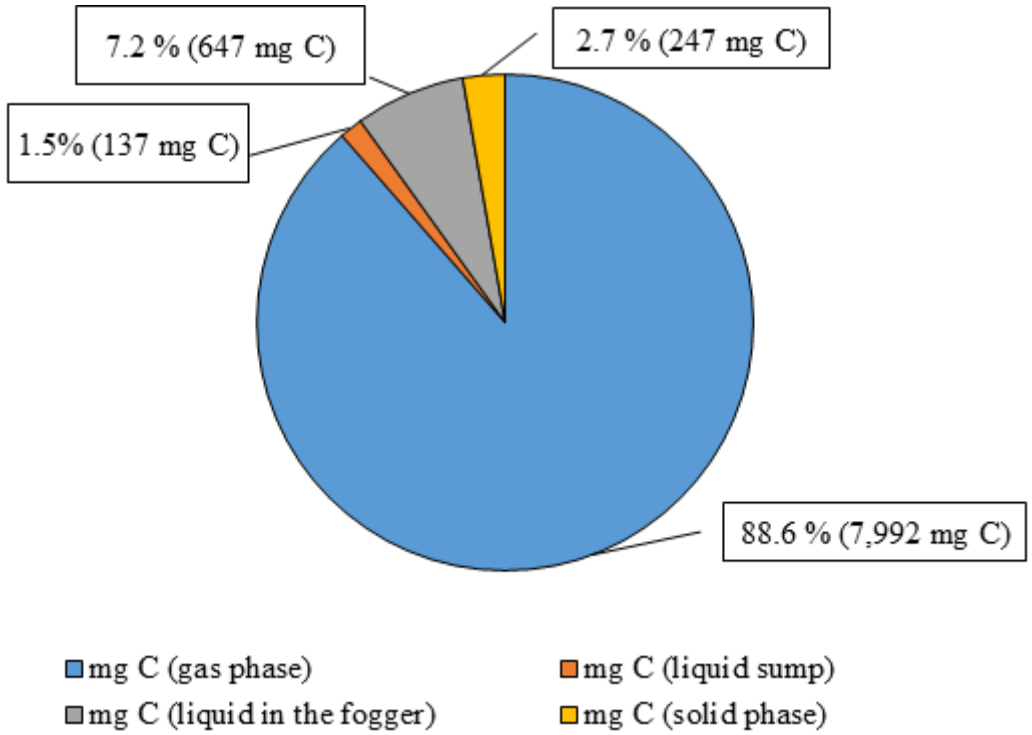

Figure S10. Percentage of carbon associated with degraded toluene at different endpoints in a DBTF system.

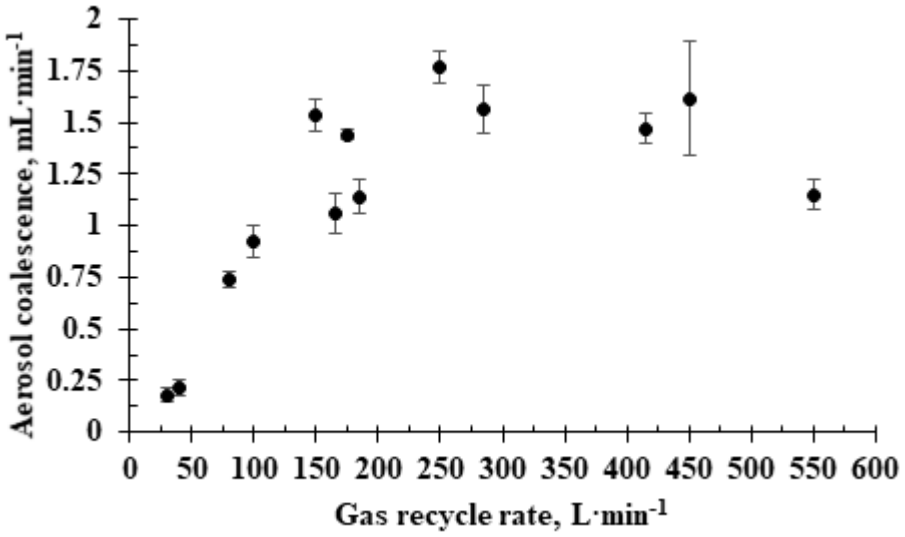

Figure S11. The aerosol coalescence rate vs. gas recycle rate at a 50-mm bed thickness.

Supplemental information 3

Estimation of elimination capacity in a BTF with 2-mm glass beads and 5-mm glass beads as packing material

A. From the study of Mirpuri et al. (1997) which employed the use of a vapor phase bioreactor (VPBR) operating in a countercurrent mode, the following biofilm kinetics data were used in the estimation:

a.1 From Figure 4 of their paper, measured at the vapor inlet side,

$$\text{Biomass production} = \frac{1.4\ \text{g of biomass}}{\text{m}^2\text{of bed}}$$

a.2 From Figure 6 of their paper, at 300 ppm:

$$\text{Specific Activity of Biomass (SAB)} = \frac{0.05 \text{ mg of degraded toluene}}{\text{mg of biomass} \cdot \text{hr}}$$

a.3 From Table of Specific Surface Area (SAA) for Raschig rings (Acechempack Tower Packing Co. n.d.);

$$\text{Specific Surface Area of Raschig rings} = \frac{789 \text{ m}^2}{\text{m}^3}$$

B. Calculations

b.1 Amount of biomass that can be supported per unit volume

$$\frac{\text{Biomass}}{\text{unit volume}} = \left(\frac{1.4 \text{ g of biomass}}{\text{m}^2 \text{of bed}}\right)\left(\frac{789 \text{ m}^2}{\text{m}^3 \text{of bed}}\right) = \frac{1{,}104.6 \text{ g of biomass}}{\text{m}^3 \text{of bed}}$$

b.2 Elimination capacity

$$\text{EC} = \left(\frac{0.05 \text{ mg of degraded toluene}}{\text{mg of biomass} \cdot \text{hr}}\right)\left(\frac{1 \text{ g of toluene}}{1{,}000 \text{ mg of toluene}}\right)\left(\frac{1{,}000 \text{ mg of biomass}}{1 \text{ g of biomass}}\right)\left(\frac{1{,}104.6 \text{ g of biomass}}{\text{m}^3 \text{ of bed}}\right)$$

$$\text{EC} = \frac{55.23 \text{ g of degraded toluene}}{\text{m}^3 \text{of bed} \cdot \text{hr}}$$

b.3 Assuming the same biomass production rate per m^2 of bed and SAB with that of the Raschig rings, the EC in a BTF with 2-mm glass beads as packing material was calculated as shown below:

As specified by Merck (n.d.-a) and Merck (n.d.-b);

$$\text{Packing density of } 2-\text{mm glass beads} = \frac{1{,}262.11 \text{ kg}}{\text{m}^3}$$

$$\text{Surface Area of } 2\text{-mm glass beads} = 4\pi r^2 = 4\pi\left(1x10^{-3} \text{m}\right)^2 = 1.26x10^{-5} \text{m}^2$$

$$\text{Volume of } 2-\text{mm glass beads} = \frac{4}{3}\pi r^3 = \frac{4}{3}\pi\left(1x10^{-3} \text{m}\right)^3 = 4.19x10^{-9} \text{m}^3$$

$$\text{Specific Surface Area of 2 - mm glass beads} = \left(\frac{1.26x10^{-5}\,\text{m}^2}{4.19x10^{-9}\,\text{m}^3}\right)\left(\frac{\text{m}^3}{1{,}262.11\,\text{kg}}\right) = \frac{2.38\,\text{m}^2}{\text{kg}}$$

Expressing it in terms of $m^2 \cdot m^{-3}$;

$$\frac{\text{m}^2}{\text{m}^3} = \left(\frac{2.38\,\text{m}^2}{\text{kg}}\right)\left(\frac{1{,}262.11\,\text{kg}}{\text{m}^3}\right) = \frac{3{,}003\,\text{m}^2}{\text{m}^3}$$

$$\frac{\text{Biomass}}{\text{unit volume}} = \left(\frac{1.4\,\text{g of biomass}}{\text{m}^2\text{ of bed}}\right)\left(\frac{3{,}003\,\text{m}^2}{\text{m}^2\text{of bed}}\right) = \frac{4{,}205\,\text{g of biomass}}{\text{m}^3\text{ of bed}}$$

$$\text{EC} = \left(\frac{0.05\,\text{mg of degraded toluene}}{\text{mg of biomass}\cdot\text{hr}}\right)\left(\frac{1\,\text{g toluene}}{1{,}000\,\text{mg toluene}}\right)\left(\frac{1{,}000\,\text{mg of biomass}}{1\,\text{g of biomass}}\right)\left(\frac{4{,}205\,\text{g of biomass}}{\text{m}^3\text{ of bed}}\right)$$

$$\text{EC} = \frac{210.3\,\text{g of degraded toluene}}{\text{m}^3\text{ of bed}\cdot\text{hr}}$$

For 5-mm glass beads:

$$\text{Surface Area of 5 - mm glass beads} = 4\pi r^2 = 4\pi\left(2.5x10^{-3}\,\text{m}\right)^2 = 7.85x10^{-5}\,\text{m}^2$$

$$\text{Volume of 5 – mm glass beads} = \frac{4}{3}\pi r^3 = \frac{4}{3}\pi\left(2.5x10^{-3}\,\text{m}\right)^3 = 6.55x10^{-8}\,\text{m}^3$$

$$\text{Specific Surface Area of 5 - mm glass beads} = \left(\frac{7.85x10^{-5}\,\text{m}^2}{6.55x10^{-8}\,\text{m}^3}\right)\left(\frac{\text{m}^3}{1{,}262.11\,\text{kg}}\right) = \frac{0.95\,\text{m}^2}{\text{kg}}$$

Expressing it in terms of $m^2 \cdot m^{-3}$;

$$\frac{\text{m}^2}{\text{m}^3} = \left(\frac{0.95\,\text{m}^2}{\text{kg}}\right)\left(\frac{1{,}262.11\,\text{kg}}{\text{m}^3}\right) = \frac{1{,}198\,\text{m}^2}{\text{m}^3}$$

$$\frac{\text{Biomass}}{\text{unit volume}} = \left(\frac{1.4\,\text{g of biomass}}{\text{m}^2\text{ of bed}}\right)\left(\frac{1{,}198\,\text{m}^2}{\text{m}^2\text{of bed}}\right) = \frac{1{,}677\,\text{g of biomass}}{\text{m}^3\text{ of bed}}$$

$$EC = \left(\frac{0.05 \text{ mg of degraded toluene}}{\text{mg of biomass} \cdot \text{hr}} \right) \left(\frac{1 \text{ g toluene}}{1{,}000 \text{ mg toluene}} \right) \left(\frac{1{,}000 \text{ mg of biomass}}{1 \text{ g of biomass}} \right) \left(\frac{1{,}667 \text{ g of biomass}}{\text{m}^3 \text{ of bed}} \right)$$

$$EC = \frac{84 \text{ g of degraded toluene}}{\text{m}^3 \text{ of bed} \cdot \text{hr}}$$

C. Summary

Table S1. Summary of estimated biomass density and elimination capacity in three different packing materials.

PACKING MATERIALS	**Biomass per unit volume** $\left(\frac{g_{biomass}}{m^3_{bed}} \right)$	**Elimination Capacity** $\left(\frac{g_{toluenedegraded}}{m^3_{bed} hr} \right)$
Raschig rings (1/4 in o.d. and ¼ in.long)	1,105.0[a]	55.0[a]
2-mm glass beads	4,205.0	210.3
5-mm glass beads	1,677.0	84.0

[a] value obtained from Mirpuri et al. (1997).